scraped from the surface of dish in the presence of PBS. The cell suspension was homogenized for 1 min. Lysates were centrifuged for 10 min at 13,000× *g*, the supernatants were collected, and the protein content in the samples was measured using a microbicinchoninic acid (BCA) assay (Pierce Chemical Co., Rockford, IL). CPK activity was measured with an automated analyzer, DRI-CHEM 3500 (Fuji Film Inc., Ashigara, Kanagawa). We calculated the activity of CPK (units per milligram of protein) after correction of total protein.

Immunoblot analysis

Total cellular protein extracts were prepared from whole gastrocnemius muscle or by rinsing cultures with PBS, then scraping the cells directly into sample buffer [25]. Protein concentration was determined by BCA assay. Protein was analyzed by sodium dodecyl sulfate–polyacrylamide gel electrophoresis (SDS–PAGE) and transferred to polyvinylidene fluoride membranes (Millipore Corp., Bedford, MA). Membranes were blocked with Odyssey Blocking Buffer (LI-COR Biosciences, Inc., Lincoln, NE) and incubated for 1 h with rabbit polyclonal anti-HIF-1α antibody (ZMD.417; Zymed Laboratories, Inc., South San Francisco, CA), anti-HSP90 antibody (SPC-104; Stressmarq Biosciences Inc., Victria, BC), anti-myogenin antibody (M225; Santa Cruz Biotechnology, Inc., Santa Cruz, CA), anti-β tubulin antibody (ab6046; Abcam Inc., Cambridge, MA), rabbit monoclonal anti-pan-Akt1 antibody (clone Y89; Epitomics Inc., Burlingame, CA), anti-phospho-Akt1^{Ser473} antibody (clone EP2109Y; Epitomics), anti-Bcl-2 antibody (clone E17; Epitomics), anti-Bax antibody (clone E63; Epitomics), anti-glyceraldehyde-3-phosphate dehydrogenase (GAPDH) antibody (clone EPR1977Y; Epitomics), mouse monoclonal anti-MyoD antibody (clone 5.8A; DakoCytomation Inc., Carpinteria, CA), anti-sarcomeric myosin heavy chain (sMyHC) antibody [clone MF20; Developmental Studies Hybridoma Bank (DSHB), Iowa City, IA], anti-pan-p38α/SAPK2α antibody (612168; BD Transduction Laboratories), anti-phospho-p38MAPK$^{Thr180/Tyr182}$ antibody (612280; BD Transduction Laboratories), anti-ERK1 antibody (610030; BD Transduction Laboratories, Lexington, KY), anti-phospho-ERK1/2$^{Thr202/Tyr204}$ antibody (612358; BD Transduction Laboratories), anti-pan-JNK/SAPK1 antibody (610627; BD Transduction Laboratories), and anti-phospho-JNK$^{Thr183/Tyr185}$ antibody (612540; BD Transduction Laboratories). Membranes were washed and incubated with goat anti-rabbit IgG antibody conjugated with Alexa Fluor 680 (Molecular Probes Inc., Eugene, OR) and rabbit anti-mouse IgG antibody conjugated with IRDye800 (Rockland Immunochemicals Inc., Gilbertsville, PA) and analyzed with an Odyssey Infrared Imaging System (LI-COR). Gel densitometries were quantified by using ImageJ software (Ver. 1.42, http://rsb.info.nih.gov/ij/). To verify equal loading, membranes were probed with anti-β-tubulin antibody or stained with IRDye Blue Protein Stain (LI-COR).

Immnocytochemical analysis

Cells were fixed with 3.8% paraformaldehyde, permeabilized with 0.5% TritonX-100, and then incubated with a mouse monoclonal anti-sarcomeric myosin heavy chain (sMyHC) (DSHB). After washes in PBS, primary antibody binding was visualized with goat anti-rabbit IgG antibody conjugated with goat anti-mouse IgG antibody conjugated with Alexa Fluor 594 (Molecular Probes) for 30 min before washing and mounting in fluorescent mounting medium (DakoCytomation) containing Hoechst 33258. The fusion index is defined as the percentage of nuclei present in myotubes (>2 nuclei) compared with the total number of nuclei present in the observed field. The diameter of myotubes was measured using ImageJ software (National Institutes of Health, Bethesda, MD; available at http://rsb.info.nih.gov/ij/). The average diameter *per* myotube was calculated as the mean of five measurements taken along the length of the myotube. The length of myotube was measured.

Identification of apoptotic nuclei

To confirm the presence of DNA cleavage, which characteristically occurs in apoptotic cells, we identified apoptotic nuclei in the presence or absence of geldanamycin. Apoptotic nuclei were detected by a terminal deoxynucleotidyl transferase (TdT) dUTP nick-end labeling (TUNEL) method using In situ Apoptosis Detection Kit (TaKaRa Bio, Inc., Otsu, Shiga). The cells were fixed in 4% paraformaldehyde, permeabilized with 0.1% Triton X-100 in 0.1% sodium citrate, and incubated with TdT and fluorescein-dUTP at 37°C for 60 min. Nuclei were counterstained with propidium iodide (Sigma-Aldrich). Apoptotic nuclei frequency was evaluated as the percentage of cells/1000 nuclei.

Histochemical analysis

The tissues were transversely sectioned at 8 μm using a cryostat at −20°C and thawed on 3-amino propylethoxysilane-coated slides. The sections were fixed with 4% paraformaldehyde for 10 min. The sections were washed with PBS, blocked with PBS containing 5% bovine serum albumin and 0.1% Igepal (Sigma-Aldrich, Inc. St. Louis, MO), and then incubated overnight at 4°C with a rabbit polyclonal anti-HSP90 antibody (Stressmarq Biosciences). The sections were incubated with goat anti-rabbit IgG antibody conjugated with goat anti-rabbit IgG antibody conjugated with Alexa Fluor 594 (Molecular Probes) for

30 min at room temperature. The sections were stained with Hoechst 33258 (Sigma-Aldrich). For negative control, the sections were processed in the same way, except that the primary antibody was omitted (Data not shown). The sections were stained with hematoxylin and eosin for evaluation of general muscle architecture. For morphometrical analysis, randomly selected fields were photographed (original magnification, X100; six fields per sample). Areas occupied by myofibers or non-myofibers and fiber cross-sectional area were determined using ImageJ software.

Statistical analysis

Data are means ± standard deviation (SD). Unpaired Student's *t*-test was used to determine significance. The level of significance was set at $P < 0.05$.

Result

Effects of geldanamycin on the expression levels of HSP90 client protein, HIF-1α, in differentiating C2C12 cells

The benzoquinone ansamycin antibiotics, geldanamycin, are characterized by its ability to specifically bind to and disrupt the function of the chaperone protein HSP90, leading to the depletion of multiple oncogenic client proteins. Since HIF-1α has shown to be a HSP90 client protein [26], we examined the effects of geldanamycin on the expression levels of HIF-1α in differentiating C2C12 cells. Upon reaching confluence, C2C12 cells were cultured in differentiation medium with 20 nM geldanamycin or its vehicle solvent DMSO for 24 h or 96 h, and then total cellular extract was prepared for HIF-1α expression levels by immunoblot analysis. The amount of HIF-1α in differentiating C2C12 cells treated with geldanamycin was decreased compared with that in differentiating C2C12 cells treated with DMSO after 24 h and 96 h (Fig. 1).

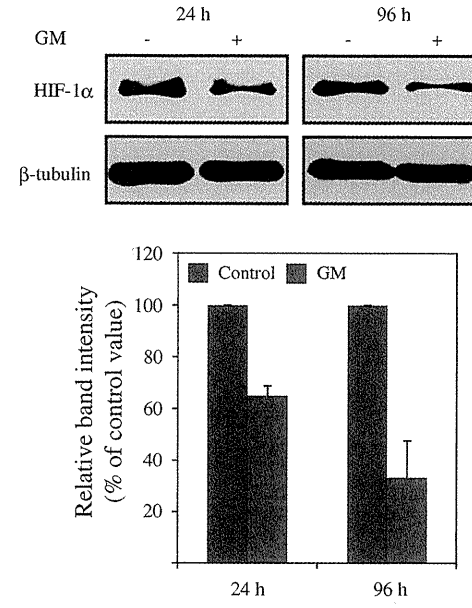

Fig. 1 Effects of geldanamycin treatment on expression levels of HSP90 client protein, HIF-1α, in differentiating C2C12 cells. Confluent cells were cultured in differentiation medium with DMSO or geldanamycin (GM) for 24 h or 96 h. The expression levels of HIF-1α were determined by immunoblot analysis with anti-HIF-1α antibody. Histograms represent the changes in the expression levels of HIF-1α. β-Tubulin was used as a loading control. The intensities of bands were measured and normalized to the control (DMSO) values. The data are the means ± SD ($n = 3$)

Pharmacological inhibition of HSP90 activity suppresses myogenic differentiation

Mouse C2C12 myoblasts have been widely used as an in vitro model to investigate the regulatory mechanisms underlying myogenic differentiation [27]. Myogenic differentiation is associated with a large increase in protein synthesis of muscle-specific proteins and enzymes involved in muscle contractions [28, 29]. To examine the effect of pharmacological inhibition of HSP90 activity on the amount of total cellular proteins during myogenic differentiation, we measured the amount of total cellular protein extracted from the C2C12 cells cultured in the presence or absence of geldanamycin. In contrast to untreated C2C12 cells, an increase in the amount of protein associated with myogenic differentiation was severely suppressed in the treated C2C12 cells (Fig. 2a). The amount of protein in the treated C2C12 cells was less than half of that in the untreated C2C12 cells 96 h after the initiation of myogenic differentiation. To quantify differentiation, the rate of muscle CPK activity was measured as a parameter of terminal myogenic differentiation. The CPK activities in the treated C2C12 cells were significantly lower than that in the untreated C2C12 cells 96 h after the initiation of myogenic differentiation (Fig. 2b). We also examined the effects of geldanamycin on the expression of sMyHC, another terminal differentiation marker. In the untreated C2C12 cells, the expression levels of sMyHC increased to a peak 96 h after the initiation of myogenic differentiation, whereas in the treated C2C12 cells, that of sMyHC was observed at 72 h but severely suppressed (Fig. 2c). To further characterize the inhibitory effect of geldanamycin on myogenic differentiation, we immunohistochemically examined expression of sMyHC in C2C12 cells cultured in differentiation medium after 96 h. As expected, the treatment of geldanamycin dramatically blocked myotube formation. The myotubes cultured in the presence of geldanamycin were shorter and thinner than

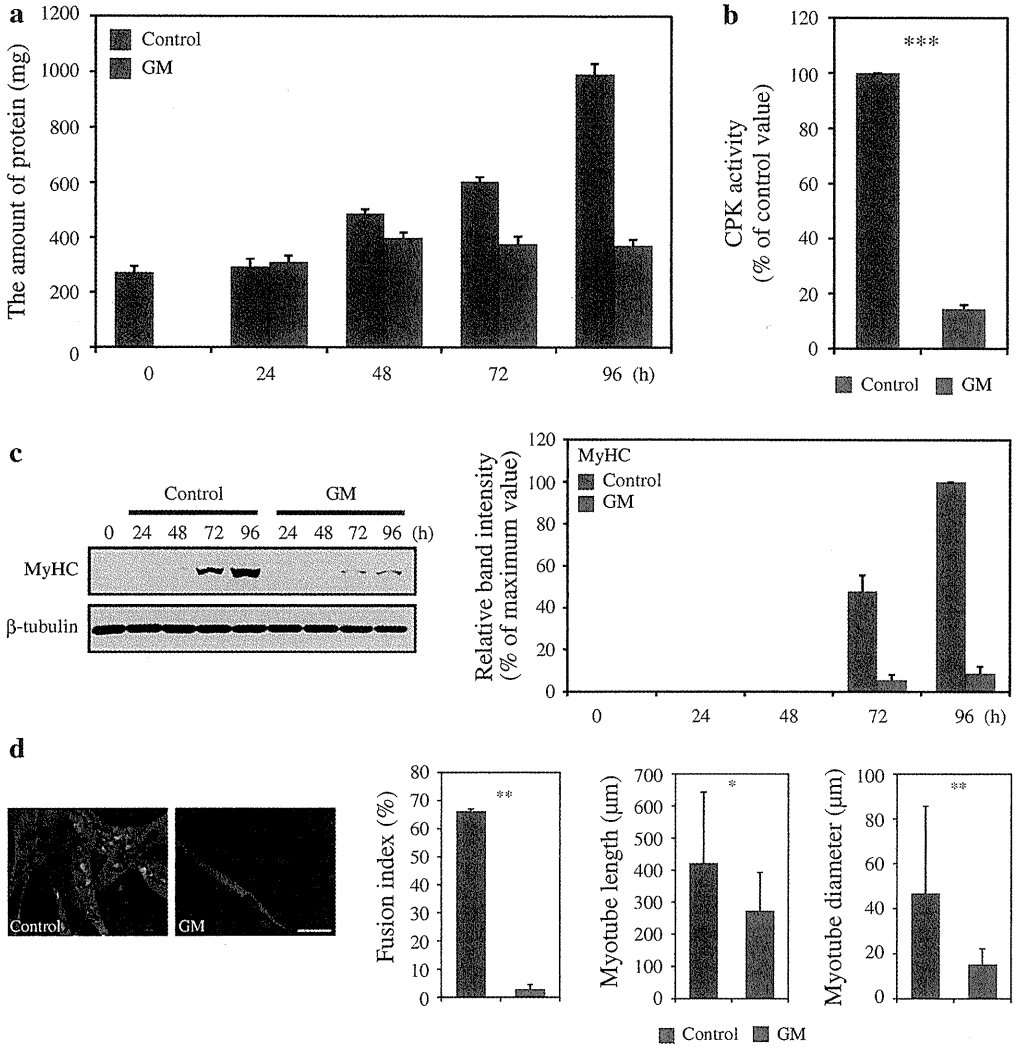

Fig. 2 Effects of geldanamycin treatment on the amount of total protein, CPK activity, and on expression levels of sMyHC protein during myogenic differentiation. Cells maintained in differentiation medium were treated with DMSO or geldanamycin for the time indicated in the figure (24-96 h). **a** Cells were harvested at 0, 24, 48, 72, or 96 h, and protein concentration was determined by BCA assay. Histogram represents the temporal changes in the amount of total protein during myogenic differentiation ($n = 3$/time point). **b** The CPK activity was measured with an automated analyzer at 96 h after induction of myogenic differentiation. Histogram represents relative changes in CPK activity. The data are expressed as a percentage change relative to control value arbitrary set to 100%. The data are the means ± SD of at least six independent experiments. **c** The level of sMyHC was determined by immunoblot analysis with anti-sMyHC antibody. Histogram represents the temporal changes in expression of sMyHC protein during myogenic differentiation ($n = 3$/time point). β-Tubulin was used as a loading control. The intensities of bands were measured and normalized to the maximum value observed during 4 days in culture. **d** For immunocytochemical analysis, the cells were cultured for 96 h and then fixed with paraformaldehyde. The cells were stained with anti-sMyHC, and nuclei were counterstained with Hoechst 33258. *Scale bar* = 100 μm. Histogram represents fusion index (nuclei inside myotubes/total number of nuclei), myotube length, or diameter ($n = 6$). The myotube length and diameter were measured with the image analysis system, calibrated to transform the number of pixels (viewed on a computer monitor) into micrometers. The data are the means ± SD of at least six independent experiments. These were statistically significant differences compared to the control (Ct): $^*P < 0.05$, $^{**}P < 0.01$, $^{***}P < 0.001$

those in the absence of geldanamycin. The fusion index for the C2C12 cells cultured in the absence of geldanamycin was 66.3 ± 0.8%, whereas the fusion index for the C2C12 cells cultured in the presence of geldanamycin was 3.0 ± 1.5%. The myotube length and diameter were significantly decreased in geldanamycin-treated cells compared with control cells (Fig. 2d).

Pharmacological inhibition of HSP90 activity decreases the expression levels of myogenic regulatory factors MyoD and myogenin upon induction of myogenic differentiation

Myogenesis is orchestrated through a series of transcriptional controls governed by the myogenic regulatory

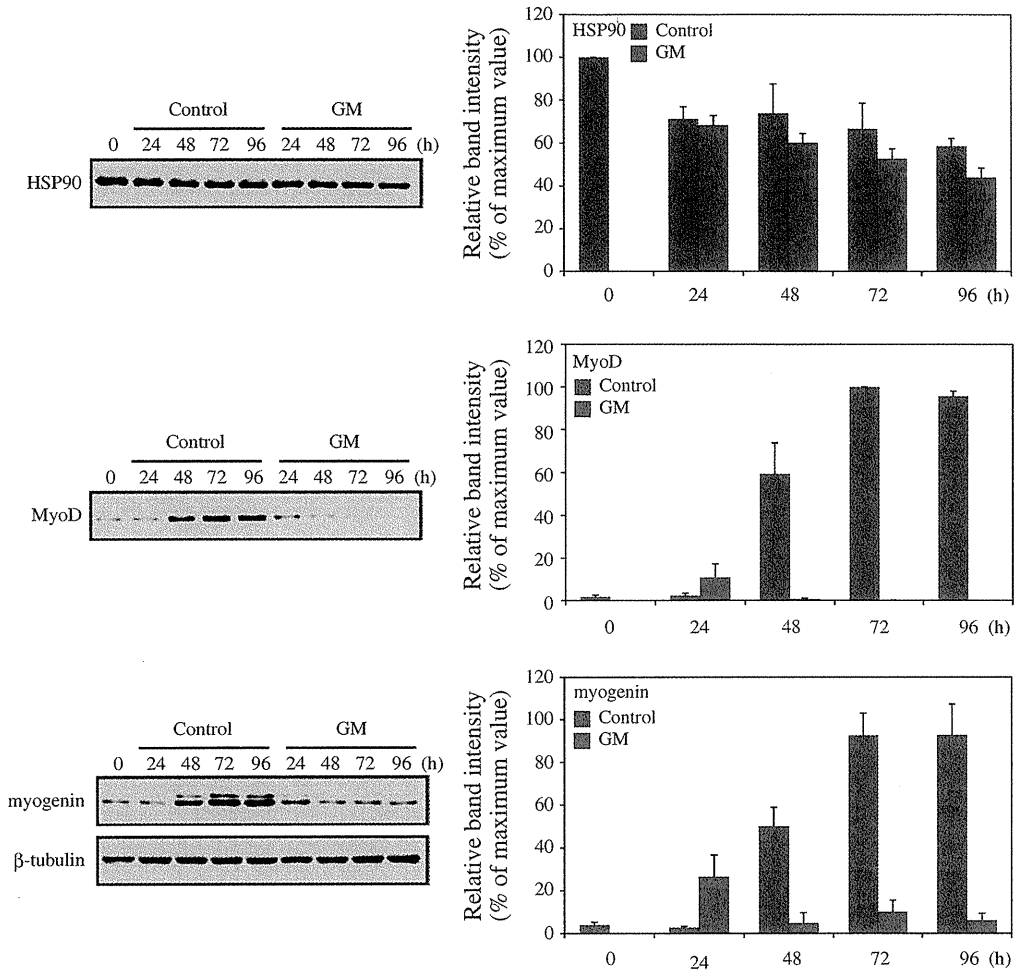

Fig. 3 Effects of geldanamycin treatment on expression of HSP90, MyoD, and myogenin proteins during myogenic differentiation. The expression levels of each protein were determined by immunoblot analysis with anti-HSP90, anti-MyoD, anti-myogenin, or anti-β-tubulin antibodies. Histograms represent the temporal changes in expression of each protein during myogenic differentiation. β-Tubulin was used as a loading control. The intensities of bands were measured and normalized to the maximum value observed during 4 days in culture. The data are the means $\pm$ SD ($n = 3$/time point)

factors. It has been well established that activated satellite cells are characterized by expression of MyoD and Myf5, whereas myoblast terminal differentiation is characterized by expression of myogenin and MRF4 [30]. We examined the effect of geldanamycin on the expression levels of MyoD and myogenin as well as HSP90 proteins during myogenic differentiation (Fig. 3). The expression levels of MyoD and myogenin proteins were gradually increased after initiation of myogenic differentiation and peaked at 72 h. The treatment of geldanamycin transiently increased the expression levels of MyoD and myogenin proteins at 24 h and then reduced the levels of these proteins during myogenic differentiation. The expression levels of HSP90 protein were slightly decreased during myogenic differentiation irrespective of geldanamycin treatment.

Pharmacological inhibition of HSP90 activity reduces phosphorylation of JNK during myogenic differentiation

Given that the extracellular signals that regulate the myogenic program are transduced to the nucleus by MAPKs [19], we examined the effect of geldanamycin on the phosphorylation levels of p38MAPK$^{Thr180/Tyr182}$, ERK1/2$^{Thr202/Tyr204}$, and JNK$^{Thr183/Tyr185}$ during myogenic differentiation (Fig. 4). As shown in Fig. 4, there were no significant differences in the phosphorylation levels of p38MAPK$^{Thr180/Tyr182}$ and ERK1/2$^{Thr202/Tyr204}$ proteins between control and geldanamycin treatment. The phosphorylation levels of JNK$^{Thr183/Tyr185}$ protein were decreased when the cells were cultured in the presence of geldanamycin. There were no significant differences in the expression levels of p38MAPK, ERK1/2, and JNK proteins between control and geldanamycin treatment.

Pharmacological inhibition of HSP90 activity reduces abundance and phosphorylation of Akt1 during myogenic differentiation

The serine/threonine kinase Akt, also known as protein kinase B (PKB), can substitute for phosphatidylinositol-3-kinase (PI3K) in the stimulation of myogenesis, and it may be an essential downstream component of PI3K-induced myogenic differentiation [10]. During myogenic differentiation, Akt

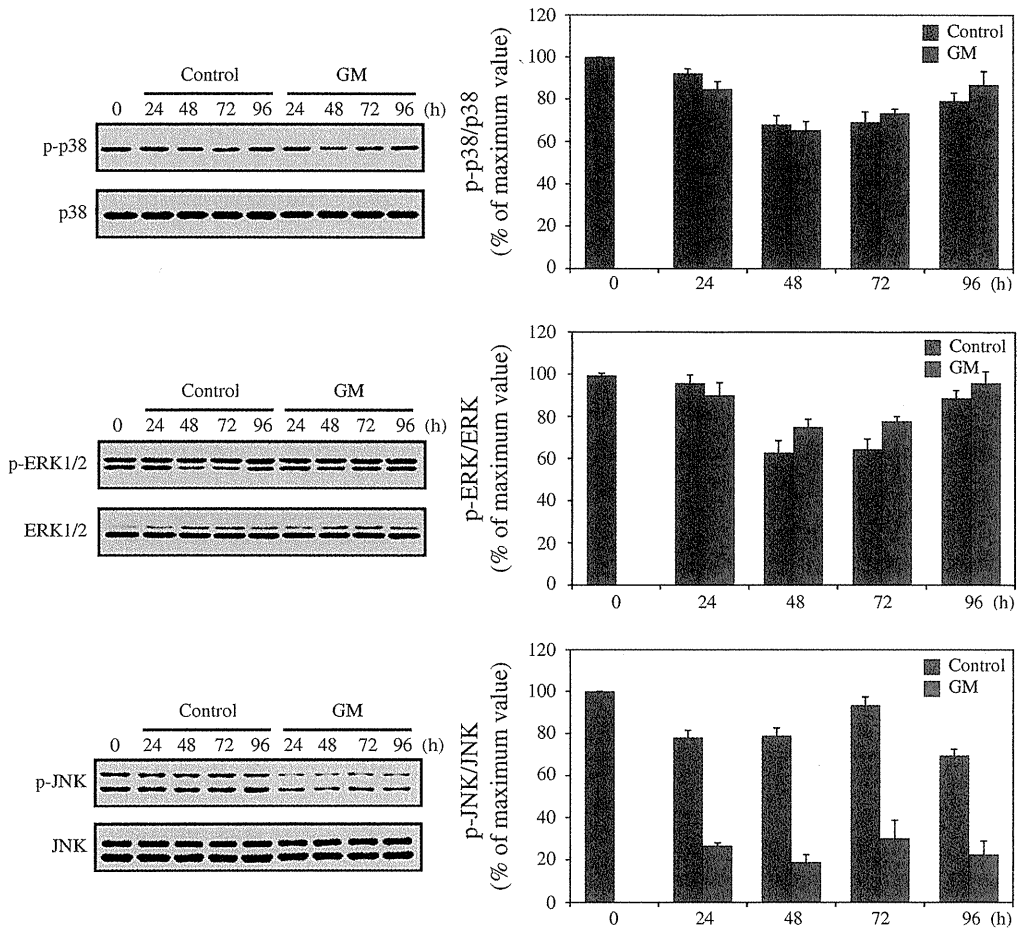

Fig. 4 Effects of geldanamycin treatment on levels of phosphorylated p38MAPK$^{Thr180/Tyr182}$, ERK1/2$^{Thr202/Tyr204}$, and JNK$^{Thr183/Tyr185}$ proteins during myogenic differentiation. Histograms represent the temporal changes in levels of p38MAPK$^{Thr180/Tyr182}$/p38MAPK, phosphorylated ERK1/2$^{Thr202/Tyr204}$/ERK1/2, and JNK$^{Thr183/Tyr185}$/JNK during myogenic differentiation. The intensities of bands were measured and normalized to the maximum value observed during 4 days in culture. The data are the means ± SD (n = 3/time point)

kinase activity correlated with Ser473 but not Thr308 phosphorylation [31]. Therefore, we examined the effect of geldanamycin on the phosphorylation levels of Akt1^{Ser473} protein during myogenic differentiation (Fig. 5). The phosphorylation levels of Akt1^{Ser473} protein increased to a peak at 72 h, followed by a decrease at 96 h in the untreated C2C12 cells. The treatment of geldanamycin gradually reduced phosphorylation levels of Akt1^{Ser473} protein during myogenic differentiation. The expression levels of Akt1 protein also decreased in the treated C2C12 cells. The ratio of phosphorylated Akt1^{Ser473} to Akt1 was gradually increased in the geldanamycin-treated C2C12 cells. This indicated that the amount of Akt1 protein decreased greater than that of phosphorylated Akt1^{Ser473}, resulting in increasing ratio of pAkt1-^{Ser473} to Akt1.

Pharmacological inhibition of HSP90 activity induces apoptosis during myogenic differentiation

Akt also enhances the survival of cells by blocking the function of proapoptotic proteins and processes [32]. Therefore, decreased phosphorylation levels of Akt1 might be expected to induce apoptotic cell death in C2C12 cells. We examined the frequency of apoptotic nuclei in the C2C12 cells treated with geldanamycin for 96 h using TUNEL method, which marks cells in a relative late phase of apoptosis. TUNEL-positive nuclei were significantly increased in the treated C2C12 cells compared with the untreated C2C12 cells (Fig. 6a). To evaluate whether a deregulated balance between pro-apoptotic and anti-apoptotic proteins could contribute to the observed apoptosis in the treated C2C12 cells, the expression levels of Bcl-2-family proteins were examined. As shown in Fig. 6b, the expression levels of anti-apoptotic Bcl-2 protein in the treated C2C12 cells were very low compared with that in the untreated C2C12 cells. In contrast, the expression levels of pro-apoptotic Bax protein in the treated C2C12 cells were nearly equivalent to that in the untreated C2C12 cells. The ratio of Bcl-2 to Bax is important in determining susceptibility to apoptosis [33]. As expected, the ratio of Bcl-2 to Bax in the treated C2C12 cells was extremely low compared with that in the untreated C2C12 cells.

The geldanamycin derivative, 17-allylamino-17-demethoxygeldanamycin (17-AAG), also decreases the expression levels of HIF-1α, myogenic regulatory factors MyoD and myogenin, and Akt1

17-AAG is a less-toxic derivative of the geldanamycin and is now in clinical trial. We used 17-AAG to further confirm

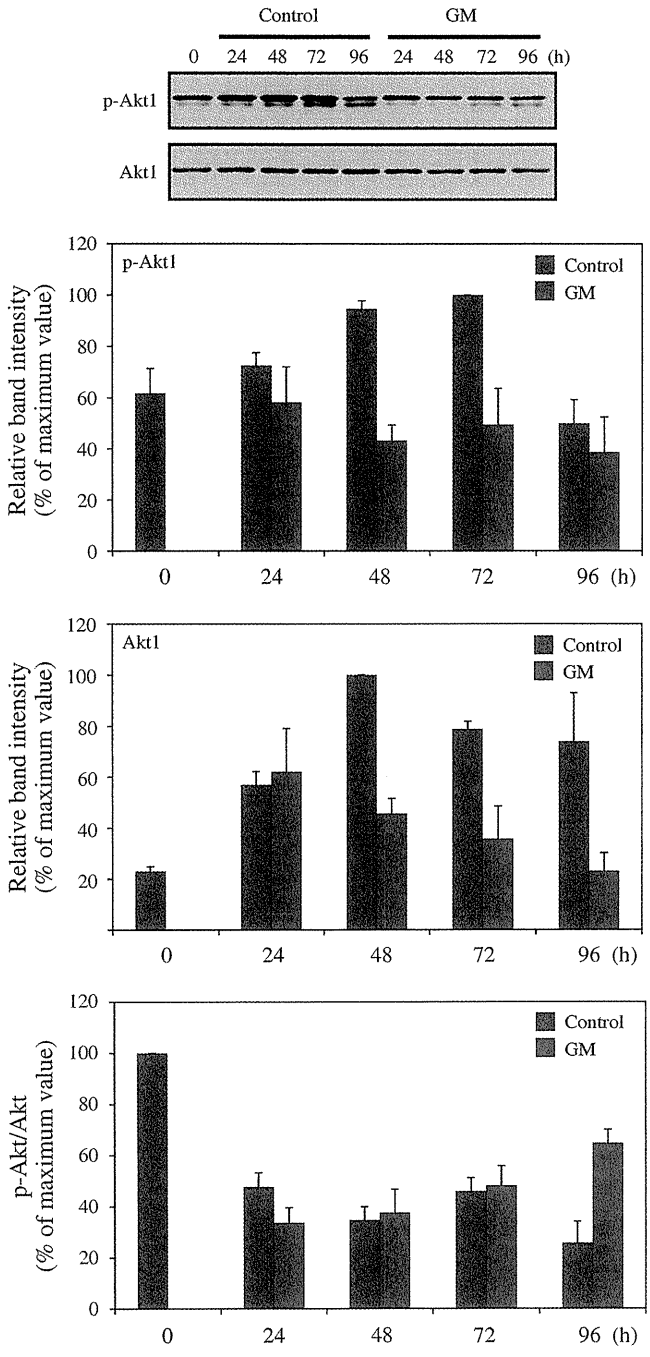

Fig. 5 Effects of geldanamycin treatment on levels of phosphorylated Akt1^{Ser473} and total Akt1 proteins during myogenic differentiation. Histograms represent the temporal changes in levels of phosphorylated Akt1^{Ser473}, total Akt1 proteins, or phosphorylated Akt1^{Ser473}/Akt1 during myogenic differentiation. The intensities of bands were measured and normalized to the maximum value observed during 4 days in culture. The data are the means ± SD (n = 3/time point)

that inhibition of HSP90 activity by geldanamycin is the cause for lower expression levels of its client proteins and myogenic regulatory factors in C2C12 cells. C2C12 cells were cultured in differentiation medium for 48 h and then treated with 17-AAG (250 nM) for 24 h. After treatment of 17-AAG, total cell lysates were prepared, and immunoblot analysis was performed with antibodies against the individual proteins. The levels of HIF-1α, MyoD, myogenin, and Akt1 were decreased in the 17-AAG-treated cells compared with in the untreated cells (Fig. 7).

Up-regulation of HSP90 coincides with increased expression of myogenic regulatory factors MyoD and myogenin during muscle degeneration/regeneration

It has been reported that up-regulation of HSP90 is observed in regenerating myofibers from patients with Duchenne muscular dystrophy [34], indicating that HSP90 expression may be regulated during myogenesis in vivo. Therefore, we monitored the temporal expression levels of HSP90, MyoD, and myogenin proteins during muscle regeneration. Muscle regeneration in gastrocnemius muscle was induced following injection of glycerol, which causes extensive and reproducible muscle necrotic injury. The myogenic differentiation is initiated within 2 days followed by extensive regeneration within 7-14 days after initiation of muscle injury [24]. Figure 8a shows the temporal changes in the amount of HSP90, MyoD, and myogenin proteins during muscle regeneration. A quantitative analysis showed that the amount of HSP90 protein increased to a peak at day 5, followed by a progressive decrease by day 14, and returned to the control level by day 28. The pattern of temporal changes in MyoD and myogenin protein levels was similar to that observed in the HSP90, exhibiting the same strong increase in day 5.

Localization of HSP90 protein in regenerating myofibers

To examine the cellular localization of the HSP90 protein during muscle degeneration/regeneration induced by injection of glycerol, immunocytochemical analysis was performed. Figure 8b shows HSP90 protein localization during muscle degeneration/regeneration. The HSP90 protein was mainly localized in nuclei of newly formed regenerating myofibers, a hallmark of regenerated myofibers, and also in mononuclear cells. The expression of HSP90 protein appeared to attenuate as myofibers, which further differentiated at later time points but was still detected in the regenerating myofibers.

Pharmacological inhibition of HSP90 activity affects muscle regeneration

To extend the results from cultured cells, we used muscle degeneration/regeneration model to examine the effect of geldanamycin on myogenic differentiation in vivo. Glycerol was injected into gastrocnemius muscles of control and

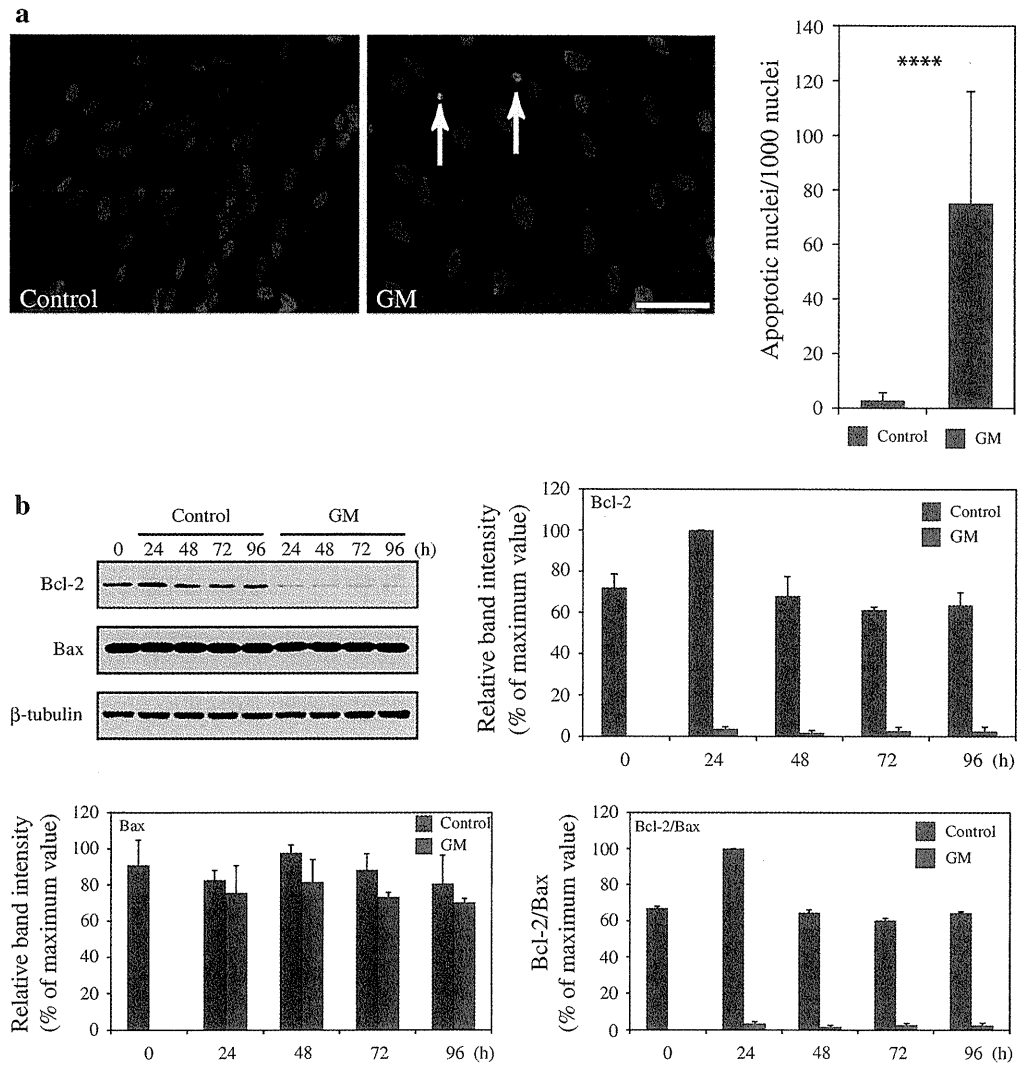

Fig. 6 Effects of geldanamycin treatment on apoptosis induction and expression of Bcl-2 and Bax proteins during myogenic differentiation. **a** The incidences of apoptotic nuclei (*arrows*) were detected by TUNEL method. Histogram represents the number of TUNEL-positive nuclei at 96 h. The data are the means ± SD of at least six independent experiments. **b** Histograms represent the temporal changes in the expression levels of each protein during myogenic differentiation. β-Tubulin was used as a loading control. The intensities of bands were measured and normalized to the maximum value observed during 4 days in culture. The data are the means ± SD (n = 3/time point). These were statistically significant differences compared to the control (Ct): $^{***}P < 0.001$

geldanamycin-treated mice. Ten days after initial injury, the muscles were removed, cryosectioned, and stained with hematoxylin and eosin. The control muscles contained numerous nascent myofibers with centrally located nuclei, whereas the skeletal muscles forced to regenerate in the presence of geldanamycin to inhibit the activity of HSP90 were of poor repair with small myofibers and increased connective tissues (Fig. 9a). A quantitative analysis showed that the area occupied by myofibers significantly decreased by 43% whereas the area occupied by non-myofibers was significantly increased by 284% in skeletal muscle when treated with geldanamycin (Fig. 9b). FCSA for regenerating myofibers was also significantly decreased by 62% (Fig. 9b). To elucidate the inhibitory effect of geldanamycin on muscle regeneration, we examined the expression levels of myogenic regulatory factors, MyoD and myogenin proteins. Total cellular protein extract was prepared at 7 days after induction of muscle injury, and immunoblot analysis was performed with antibodies against the individual proteins. The expression levels of MyoD and myogenin were decreased in the geldanamycin-treated mice compared with in the untreated mice (Fig. 9c).

Discussion

HSP90 plays some roles in cell differentiation and survival in a variety of cell types [35] including myogenic cells [8]. HSP90 activity has shown to be inhibited by geldanamycin as follows: Geldanamycin binds to conserved binding

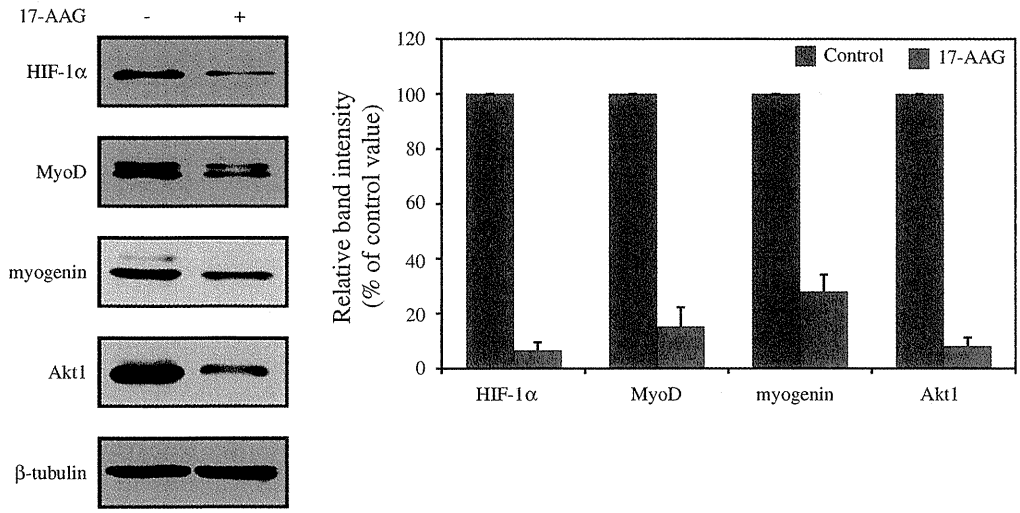

Fig. 7 Effects of geldanamycin derivative, 17-AAG, on HIF-1α, MyoD, myogenin, and Akt 1 proteins in the developing C2C12 cells. Cells were cultured with differentiation medium for 48 h and then treated with 17-AAG (250 nM) for 24 h. The expression levels of each protein were determined by immunoblot analysis with anti-HIF-1α, anti-MyoD, anti-myogenin, and anti-Akt1 antibodies. Histograms represent the relative changes in expression of each protein. β-Tubulin was used as a loading control. The intensities of bands were measured and normalized to the control value. The data are the means ± SD ($n = 3$)

pocket in the N-terminal domain of HSP90, inhibiting ATP binding and ATP-dependent release of the client proteins undergoing refolding from HSP90, leading to degradation of the client proteins by the ubiquitin-dependent proteasome pathway [36]. In this study, we examined the effect of pharmacological inhibition of HSP90 activity using geldanamycin on myogenic differentiation and cell survival in C2C12 cells. We demonstrated that myogenic differentiation was suppressed with decreased expression of myogenic regulatory factors, MyoD and myogenin, when the cells were cultured in the presence of geldanamycin. Phosphorylation levels of Akt and JNK, which are required for myogenic differentiation, were reduced in geldanamycin-treated cells compared with control cells. Confirming the results from cultured cells using in vivo model for muscle regeneration, mice treated with geldanamycin exhibited poor repair of muscle injury. Along with myogenic differentiation, apoptotic nuclei were increased in geldanamycin-treated cells compared with untreated cells with decreased expression of anti-apoptotic protein, Bcl-2. Together, our findings indicate that pharmacological inhibition of HSP90 activity may negatively modulate myogenic differentiation and may induce apoptotic cell death.

Our results extend observations from previous study [8], which has shown that geldanamycin blocks myotube formation, by providing more quantitative support for their data. Our result revealed a marked reduction in fusion capacity with only 3% nuclei being incorporated into the small myotubes in geldanamycin-treated cells. This observation could be achieved with a lower dose (0.01 μg/ml) compared with a dose (0.05 μg/ml) used in previous study [Yun 2005], and even at low dose, expression of myosin heavy chain could be suppressed in geldanamycin-treated cells. Geldanamycin-mediated inhibition of myogenic differentiation might be explained, at least in part, through down-regulation of myogenic regulatory factors to produce a skeletal muscle-specific expression pattern. Some possible mechanisms for this down-regulation can be envisioned. One possibility is that MyoD may be putative target protein for HSP90. HSP90 could rapidly convert MyoD from an inactive to an active conformation, whose conversion process involves a transient interaction between HSP90 and MyoD [37]. This may be supported by our observation that HSP90 protein was localized in the nuclei of regenerating myofibers, which expresses MyoD protein [38]. On the other hand, geldanamycin-induced inhibition of HSP90 activity has little effect on interaction between MyoD and HSP90, although the interaction of MyoD with the cochaperone adaptor protein, Cdc37, is disrupted by geldanamycin [8]. Thus, it is difficult to conclude that pharmacological inhibition of HSP90 activity is directly involved in decreased expression of MyoD observed in this study. Another possibility is that pharmacological inhibition of HSP90 activity indirectly influences on expression of myogenic regulatory factors. It has been reported that Akt activity is closely linked to the expression of myogenic regulatory factors. Targeted knockdown of Akt1 leads to depletion of MyoD and myogenin in C2C12 cells [39]. In addition, dominant-negative Akt decreases transcriptional activity of MyoD, and short hairpin RNA-mediated inhibition of Akt1 results in decreased myogenin promoter activity [40]. Thus, down-regulation of myogenic regulatory factors observed in geldanamycin-treated cells may be due to depletion of Akt after induction of myogenic differentiation.

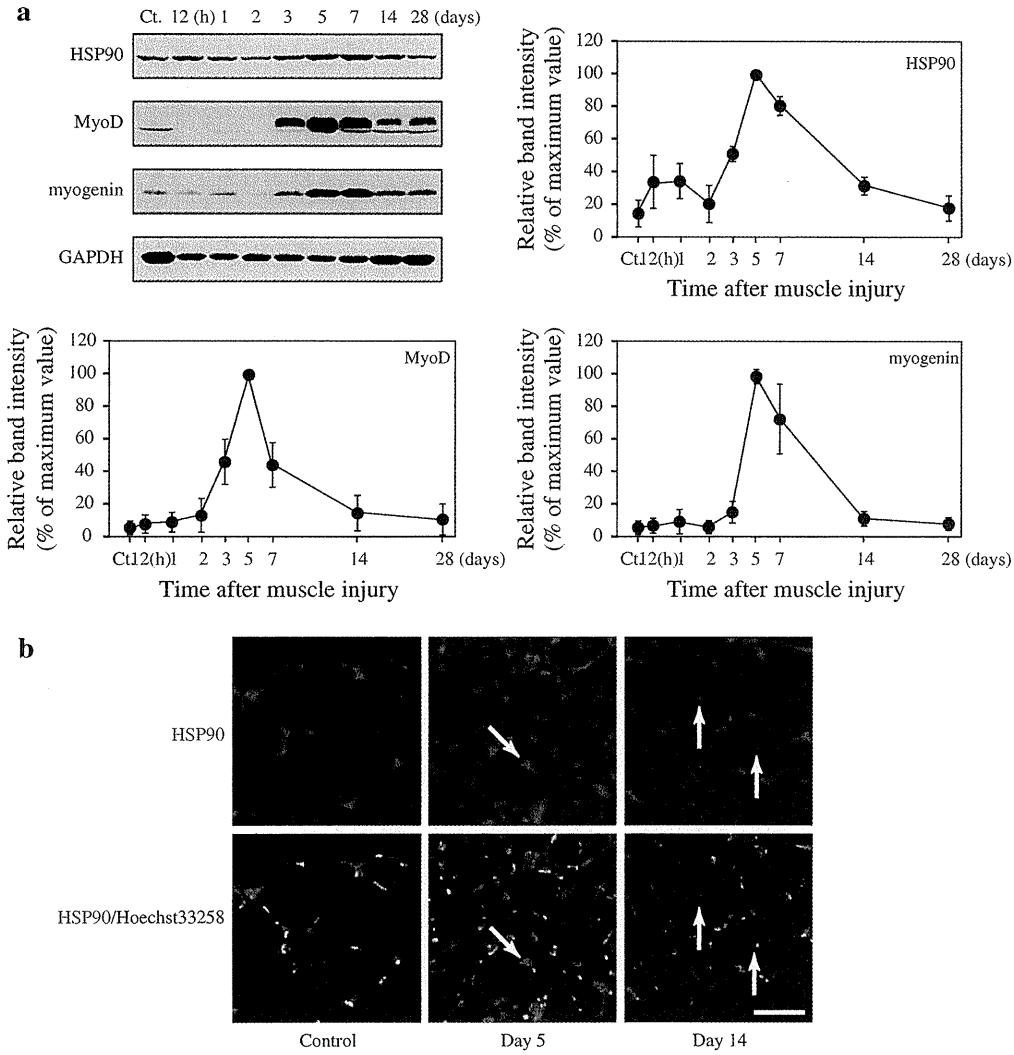

Fig. 8 Temporal changes in expression of HSP90, MyoD, and myogenin proteins during muscle degeneration/regeneration. **a** Tissues were isolated for immunoblot analysis at various time points [Control (Ct), 12 h, 1, 2, 3, 5, 7, 14, or 28 days]. Line graphs represent the temporal changes in the expression levels of each protein during myogenic differentiation. GAPDH was used as a loading control. The intensities of bands were measured and normalized to the maximum value observed during muscle degeneration/regeneration. Because of the extensive myofiber necrosis at early time points of muscle degeneration/regeneration, the amount of GAPDH was not equal across all the time points, as expected. The data are the means ± SD (n = 3/time point). **b** HSP90 protein localization on day 5 and day 14 after muscle injury. The fixed tissues were stained with anti-HSP90 antibody, and nuclei were counterstained with Hoechst 33258. Arrows indicate a nuclear localization of HSP90 protein in regenerating myofibers. All experiments were performed at least three times. *Scale bar* = 50 μm

Consistent with previous study [8], inhibition of HSP90 activity by geldanamycin resulted in progressive loss of Akt protein after induction of myogenic differentiation, likely through the ubiquitin proteasome pathway. Indeed, proteasome inhibitor, lactacystin, partially protects Akt protein from geldanamycin-mediated loss [41]. It has been shown that geldanamycin causes newly synthesized Akt protein to be degraded rapidly but has little effect on mature Akt protein in C2C12 cells [8]. Thus, geldanamycin-mediated depletion of Akt1 observed in this study appears to be due to the inability of the cells to mature newly synthesized Akt1 protein into a stable conformation.

In this study, the phosphorylation levels of $Akt1^{Ser473}$ were increased maximally at 72 h and were decreased at 96 h after induction of myogenic differentiation in untreated cells, whereas in geldanamycin-treated cells, reduced phosphorylation levels of $Akt1^{Ser473}$ were continued. This suggests that phosphorylation levels of $Akt1^{Ser473}$ may be temporally regulated to sufficient to differentiate into myoblasts and fuse to form myofibers. Akt1 is phosphorylated at two key regulatory sites, Thr308 and Ser473, by 3-phosphoinositide-dependent kinase-1 (PDK1) [42] and by mammalian target of rapamycin complex 2 (mTORC2) [43], respectively. Since Thr308 phosphorylation is necessary for

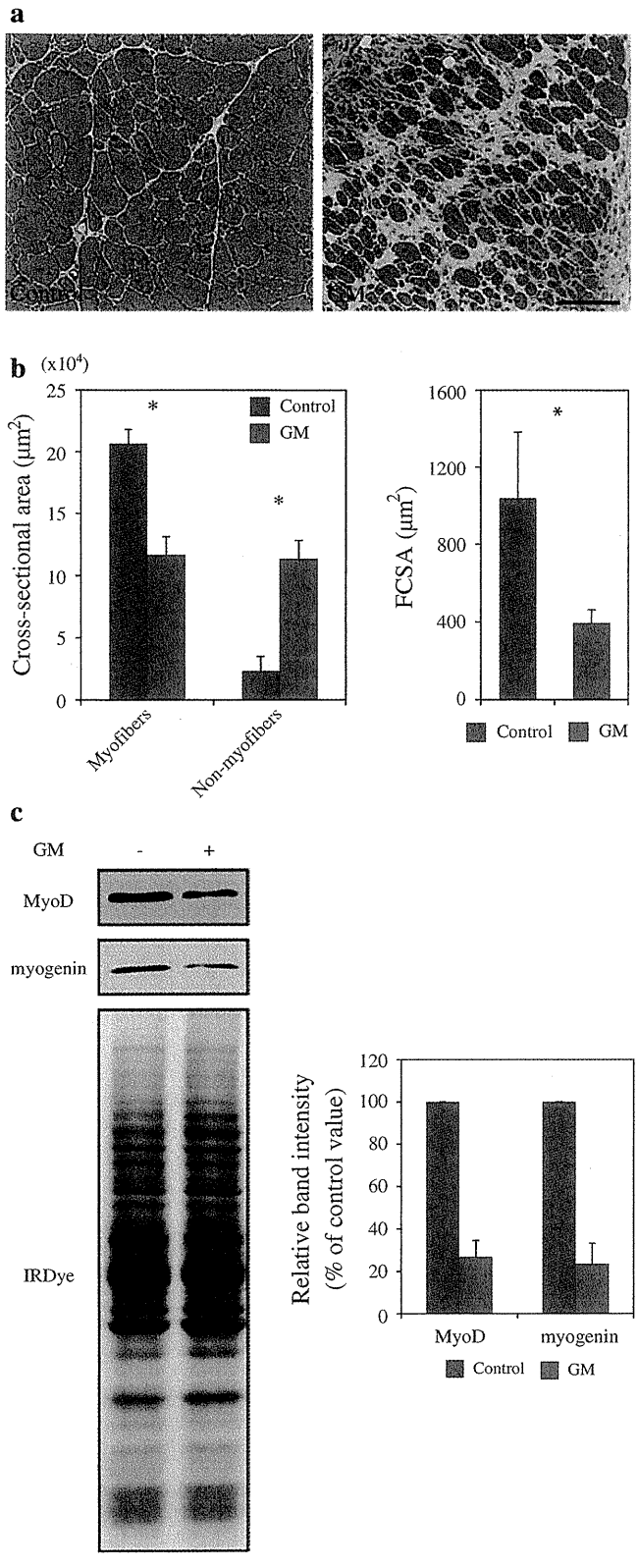

◀ **Fig. 9** Effects of geldanamycin treatment on muscle regeneration. **a** Tissues were isolated for histochemical analysis 10 days after initiation of muscle injury, fixed, sectioned, and then stained with hematoxylin and eosin. *Scale bar* = 100 μm. **b** Histograms represent the areas occupied by myofibers and non-myofibers, or FCSA. The data are the means ± SD of at least six independent experiments. These were statistically significant differences compared to the control (Ct): $^{**}P < 0.01$. **c** The expression levels of each protein were determined by immunoblot analysis with anti-MyoD and anti-myogenin antibodies. Histograms represent the relative changes in expression of each protein at day 7 after induction of muscle injury. Membranes were stained with IRDye to verify equal loading. The intensities of bands were measured and normalized to the control value. The data are the means ± SD ($n = 3$)

activation of Akt1 and Ser473 phosphorylation is only required for maximal activity [44], alterations in PDK1/mTORC2 activities could undoubtedly contribute to the decline of Akt1 activity observed in geldanamycin-treated cells. Since PDK1 has been shown to be HSP90 client protein [45], geldanamycin-mediated depletion of PDK1 may result in reduced phosphorylation levels of $Akt1^{Thr308}$. However, it is unlikely that reduced phosphorylation levels of $Akt1^{Ser473}$ observed in this study may be due to reduced mTORC2 activity, since the essential mTORC2 component, rictor, which is required for phosphorylation of Ser473 in cells [46], has not been reported to be HSP90 client protein. In addition, Akt activity is also modulated through the regulation of dephosphorylation. Protein phosphatase 2A (PP2A) has been proposed to be the most likely candidate for regulating the rate of Akt dephosphorylation [47]. It has been reported that HSP90 binding to Akt protects Akt protein from PP2A-mediated dephosphorylation, whereas detachment of Akt from HSP90 promotes the PP2A-mediated dephosphorylation of Akt [47]. Thus, reduced phosphorylation of $Akt1^{Sre473}$ observed in geldanamycin-treated cells may be due to imbalance between phosphorylation and dephosphorylation by mTORC2 and PP2A.

Unexpectedly, we observed transient up-regulation of MyoD and myogenin in geldanamycin-treated cells at 24 h after induction of myogenic differentiation. However, Yun et al. report that MyoD expression remains unchanged and myogenin could not be detected in geldanamycin-treated cells at 20 h after induction of myogenic differentiation. This is in disagreement with our results. While it is difficult to explain these contradictory data, one possibility may be changes in Akt1 activity in geldanamycin-treated cells. It is interesting to note that short-term (30 min) treatment of differentiating cells with geldanamycin does not cause any decrease in Akt and increases the levels of Akt phosphorylation at Ser^{473} but not those at Thr^{308}, which correlates with an increased phosphorylation levels of glycogen synthase kinase-3β [41]. Akt1 activity correlates to MyoD and myogenin expression during myogenic differentiation. Thus, we hypothesized that activation of Akt1 by phosphorylation at Ser^{473} may occur immediately after C2C12 cells were treated with geldanamycin, resulting in inducing MyoD and myogenin at the early stage of myogenic differentiation. Another possibility is that geldanamycin can have some side effects more or less independent of HSP90.

However, as aforementioned, the concentration used in this study is lower than that used in the previous study [8]. Thus, further study may be required to elucidate the effects of geldanamycin on the expression of myogenic regulatory factors at the early stage of myogenic differentiation.

A potentially important observation that emerged from this study was that the phosphorylated levels of JNK were decreased when the C2C12 cells were treated with geldanamycin. This study is, to the best of our knowledge, the first to deal with the potential regulation of JNK in C2C12 cells using geldanamycin. JNK has been involved in controlling diverse cellular functions, including cell proliferation, differentiation, and survival [48]. Basal JNK activity appears to be required for myogenic differentiation and cell survival. Inhibition of JNK activities by JNK inhibitor II drastically inhibits myogenic differentiation and increases apoptotic nuclei in L6E9 cells [20]. Activation of JNK is mediated by a MAP kinase module, MAPKKK (MAP3K) → MAPKK (MAP2K) → MAPK through sequential protein phosphorylation. The mixed-lineage kinases (MLKs) function as MAP3K to activate the JNK pathway [49]. MLK3 activates the JNK pathway through phosphorylation and activation of MAPK kinase 4 (MKK4) [50] and MKK7 [51]. Thus, we hypothesized that sequential activation pathway may be partially impaired, resulting in reduced phosphorylation levels of JNK in geldanamycin-treated cells. This hypothesis may be supported in part by the observation that geldanamycin decreases the endogenous level of MLK3 and abolishes TNF-mediated activation of MLK3 and JNK without affecting MKK4 and MKK7 in vitro [16]. Thus, reduced phosphorylated JNK, which is regulated possibly at the MAP3K level, may contribute to geldanamycin-mediated inhibition of myogenic differentiation and cell survival.

We could fail to observe any changes in the phosphorylation levels of ERK1/2 and p38MAPK in geldanamycin-treated cells. The exact mechanism by which geldanamycin has no effect on phosphorylation levels of p38MAPK and ERK1/2 remains unclear. The response of MAPKs to geldanamycin appears to be different according to cell type. Geldanamycin transiently activates ERK2 activity at 8-9 h after treatment but does not JNK1 activity in neuroblastoma cell line [21]. The phosphorylation levels of ERK1/2 remain unchanged at 16 h after treatment in embryonic fibroblast cell line [15]. Geldanamycin derivative, 17-AAG, also reduces the phosphorylation levels of ERK1/2, p38MAPK, and JNK at 24 h after treatment in colon cancer cell lines [52]. These results indicate that the response of MAPKs to geldanamycin may be cell-type specific, depending on the dose and time of the treatment.

It has been demonstrated that the geldanamycin-treated cells for 24 h undergo apoptosis using a marker for the initial stage of apoptosis, cleaved poly(adenosine diphosphate–ribose ribose) polymerase [8]. We also showed that apoptotic nuclei were increased in geldanamycin-treated cells using a relatively late marker, DNA fragmentation as assessed by TUNEL. To gain insight into apoptotic response of C2C12 cells to geldanamycin, we focused on the Bcl-2 family, which is the best-characterized protein family involved in the regulation of apoptotic cell death, consisting of anti-apoptotic and pro-apoptotic members. We observed decreased expression levels of Bcl-2 protein but not those of Bax in the geldanamycin-treated cells. Bcl-2 localized in the mitochondrial membrane prevents the apoptosis-associated release of cytochrome *c* [53, 54] and apoptosis-inducing factor (AIF) [55] from the mitochondrial inter-membrane space into the cytoplasm. HSP90β has been shown to associate with Bcl-2 in mast cells. Depletion of HSP90β with a siRNA or inhibition of HSP90 with geldanamycin inhibits HSP90 interaction with Bcl-2 [22]. Thus, geldanamycin may conduce to unbalanced Bcl-2/Bax ratio in C2C12 cells, resulting in release of cytochrome c, caspase activation, and/or AIF, chromatin condensation, and DNA degradation, eventually leading to apoptosis. We observed that the majority of TUNEL-positive cells were mononuclear cells treated with geldanamycin. When proliferating myoblasts are induced to differentiate by deprivation of serum in the medium, a significant proportion of cells escape from terminal differentiation. The undifferentiated cells refer to as reserve cells [56]. It has been reported that Bcl-2 is expressed at the high levels in the reserve cells whereas it is expressed at very low levels in the myotubes [57], suggesting that Bcl-2 becomes the molecular marker of reserve cells. Although the physiological role of Bcl-2 expressed in the reserve cells is not fully understood, Bcl-2-positive cells resist apoptosis and are at an early stage of a process leading from muscle progenitor cell to myotube [58]. Thus, reduced levels of Bcl-2 observed in this study may reflect the loss of reserve cells, which would be eliminated possibly through apoptosis-dependent pathway.

Although HSP90 has been shown to be expressed in regenerating myofibers, it remains unknown whether HSP90 contributes to myogenesis in vivo. Given that HSP90 is involved in myogenic differentiation, expression of myogenic regulatory factors and HSP90 would be regulated in a coordinated manner during muscle regeneration. We showed that MyoD, myogenin, and HSP90 were simultaneously up-regulated at day 5 after induction of muscle injury. In addition, HSP90 was localized in nuclei of newly formed myofibers (day 5) and still present in the nuclei of regenerating myofibers at the later stage of muscle regeneration (day 14). It has been demonstrated that MyoD and myogenin are coexpressed in newly formed myofibers and they persists in the nuclei of regenerating myofibers for at least 2 weeks [38]. Thus, MyoD, myogenin, and HSP90 may be coexpressed in the regenerating myofibers. MyoD appears to induce terminal cell cycle

arrest during myogenic differentiation by increasing the expression of cyclin-dependent kinase inhibitor, $p21^{WAF1/CIP1}$ [59]. The myogenic regulatory factors activate transcription of muscle-specific genes by binding, upon heterodimerization with ubiquitous E proteins [60], the E-box consensus sequence in skeletal muscle gene promoters and enhancers [61]. Considering their role in myogenesis, elevated levels of HSP90 in regenerating myofibers may reflect an increased demand for its basal functions during cell cycle growth arrest and/or the progressive expression of the muscle phenotype.

It is likely that geldanamycin and 17-AAG may have positive and negative effects on muscle regeneration in vivo. Kayani et al. report that 17-AAG-mediated up-regulation of HSP70 results in improved recovery of force generation in skeletal muscles of old mice following lengthening contraction-induced damage [62]. Similar results have been shown in HSP70 transgenic mice [63]. Indeed, HSP70 overexpression inhibits NF-κB transcriptional activity [64], which acts as a negative regulator of myogenic differentiation [65]. On the other hand, we showed that pharmacological inhibition of HSP90 activity impaired muscle regeneration with decreased expression levels of MyoD and myogenin in vivo. Geldanamycin treatment resulted in the decreased size of regenerating myofibers, which could partially reflect the results from cultured cells. We cannot exclude the possibility that geldanamycin may have unexpected and undesirable side effects more or less independent of HSP90. Thus, we examined the toxic side effects of geldanamycin throughout experimental period. No pathological symptoms were observed by visual inspection, and no decreases in body weight were observed at a concentration used in this study (data not shown). Thus, we believe that its side effects are minimal. Besides myofiber regeneration, pharmacological inhibition of HSP90 activity might have an impact on neuromuscular junction (NMJ) formation, which is also essential aspect of the muscle regeneration process [30]. It has been reported that HSP90β plays an important role in NMJ formation in vivo by injecting 17-AAG intraperitoneally into embryos in utero at E14.5 [66], a time when the NMJ starts to form [67]. Previous study and our results indicate that HSP90 may be involved in myogenesis as well as NMJ formation in vivo. Although geldanamycin and its derivatives may have therapeutic benefit in the recovery following muscle damage, they have also the potential adverse effect on the viability of myogenic cells through their ability to impair the function of multiple HSP90-dependent signal pathways that are critical for cell differentiation and survival.

In conclusion, pharmacological inhibition of HSP90 activity led to depletion of signal transduction proteins whose are necessary for myogenic differentiation and cell survival. As HSP90 has been found to be either overexpressed or constitutively more active in cancer cells [68], HSP90 is an emerging target in cancer treatment due to its important role in maintaining transformation and in increasing the survival and growth of cancer cells [69]. 17-AAG, which has similar antitumor activity to that of geldanamycin with less toxicity [70], is currently being tested in ongoing phase 1 and phase 2 clinical trials [71]. Our results suggest that geldanamycin showed inhibitory effects on myogenesis in vivo and in vitro, which provides information that myogenic cells were sensitive to HSP90 inhibition, depending on experimental conditions.

Acknowledgments This research was supported by the MEXT (The Ministry of Education, Culture, Sports, Science and Technology) (Grant-in Aid for Scientific Research (C), 22500658) Japan. This research was also supported in part by The Ichiro Kanehara Foundation, Comprehensive Research on Disability Health and Welfare (H22-ShinkeiKin-Ippan-016) and Nervous and Mental Disorders (20B-13) from MHLW (The Ministry of Health, Labour and Welfare) Japan.

References

1. Lindquist S (1986) The heat-shock response. Annu Rev Biochem 55:1151–1191
2. Sharp FR, Massa SM, Swanson RA (1999) Heat-shock protein protection. Trends Neurosci 22:97–99
3. Buchner J (1999) Hsp90 & Co. - a holding for folding. Trends Biochem Sci 24:136–141
4. Whitesell L, Lindquist SL (2005) HSP90 and the chaperoning of cancer. Nat Rev Cancer 5:761–772
5. Barral JM, Hutagalung AH, Brinker A, Hartl FU, Epstein HF (2002) Role of the myosin assembly protein UNC-45 as a molecular chaperone for myosin. Science 295:669–671
6. Lele Z, Hartson SD, Martin CC, Whitesell L, Matts RL, Krone PH (1999) Disruption of zebrafish somite development by pharmacologic inhibition of Hsp90. Dev Biol 210:56–70
7. Sass JB, Martin CC, Krone PH (1999) Restricted expression of the zebrafish hsp90alpha gene in slow and fast muscle fiber lineages. Int J Dev Biol 43:835–838
8. Yun BG, Matts RL (2005) Differential effects of Hsp90 inhibition on protein kinases regulating signal transduction pathways required for myoblast differentiation. Exp Cell Res 307:212–223
9. Connell P, Ballinger CA, Jiang J, Wu Y, Thompson LJ, Hohfeld J, Patterson C (2001) The co-chaperone CHIP regulates protein triage decisions mediated by heat-shock proteins. Nat Cell Biol 3:93–96
10. Jiang BH, Aoki M, Zheng JZ, Li J, Vogt PK (1999) Myogenic signaling of phosphatidylinositol 3-kinase requires the serine-threonine kinase Akt/protein kinase B. Proc Natl Acad Sci 96:2077–2081
11. Andrechek ER, Hardy WR, Girgis-Gabardo AA, Perry RL, Butler R, Graham FL, Kahn RC, Rudnicki MA, Muller WJ (2002) ErbB2 is required for muscle spindle and myoblast cell survival. Mol Cell Biol 22:4714–4722
12. Fujio Y, Guo K, Mano T, Mitsuuchi Y, Testa JR, Walsh K (1999) Cell cycle withdrawal promotes myogenic induction of Akt, a positive modulator of myocyte survival. Mol Cell Biol 19: 5073–5082
13. Laprise P, Poirier EM, Vézina A, Rivard N, Vachon PH (2002) Merosin-integrin promotion of skeletal myofiber cell survival:

differentiation state-distinct involvement of p60Fyn tyrosine kinase and p38alpha stress-activated MAP kinase. J Cell Physiol 191:69–81
14. Turjanski AG, Vaqué JP, Gutkind JS (2007) MAP kinases and the control of nuclear events. Oncogene 26:3240–3253
15. Schulte TW, Blagosklonny MV, Romanova L, Mushinski JF, Monia BP, Johnston JF, Nguyen P, Trepel J, Neckers LM (1996) Destabilization of Raf-1 by geldanamycin leads to disruption of the Raf-1-MEK-mitogen-activated protein kinase signalling pathway. Mol Cell Biol 16:5839–5845
16. Zhang H, Wu W, Du Y, Santos SJ, Conrad SE, Watson JT, Grammatikakis N, Gallo KA (2004) Hsp90/p50cdc37 is required for mixed-lineage kinase (MLK) 3 signaling. J Biol Chem 279: 19457–19463
17. Davis MA, Carbott DE (1999) Herbimycin A and geldanamycin inhibit okadaic acid-induced apoptosis and p38 activation in NRK-52E renal epithelial cells. Toxicol Appl Pharmacol 161:59–74
18. Bennett AM, Tonks NK (1997) Regulation of distinct stages of skeletal muscle differentiation by mitogen-activated protein kinases. Science 278:1288–1291
19. Wu Z, Woodring PJ, Bhakta KS, Tamura K, Wen F, Feramisco JR, Karin M, Wang JY, Puri PL (2000) p38 and extracellular signal-regulated kinases regulate the myogenic program at multiple steps. Mol Cell Biol 20:3951–3964
20. Khurana A, Dey CS (2004) Involvement of c-Jun N-terminal kinase activities in skeletal muscle differentiation. J Muscle Res Cell Motil 25:645–655
21. López-Maderuelo MD, Fernández-Renart M, Moratilla C, Renart J (2001) Opposite effects of the Hsp90 inhibitor Geldanamycin: induction of apoptosis in PC12, and differentiation in N2A cells. FEBS Lett 490:23–27
22. Cohen-Saidon C, Carmi I, Keren A, Razin E (2006) Antiapoptotic function of Bcl-2 in mast cells is dependent on its association with heat shock protein 90beta. Blood 107:1413–1420
23. Yaffe D, Saxel O (1977) Serial passaging and differentiation of myogenic cells isolated from dystrophic mouse muscle. Nature 270:725–727
24. Kawai H, Nishino H, Kusaka K, Naruo T, Tamaki Y, Iwasa M (1990) Experimental glycerol myopathy: a histological study. Acta Neuropathol 80:192–197
25. Anderson LV, Davison K (1999) Multiplex Western blotting system for the analysis of muscular dystrophy proteins. Am J Pathol 154:1017–1022
26. Minet E, Mottet D, Michel G, Roland I, Raes M, Remacle J, Michiels C (1999) Hypoxia-induced activation of HIF-1: role of HIF-1alpha-Hsp90 interaction. FEBS Lett 460:251–256
27. Blau HM, Pavlath GK, Hardeman EC, Chiu CP, Silberstein L, Webster SG, Miller SC, Webster C (1985) Plasticity of the differentiated state. Science 230:758–766
28. Shainberg A, Yagil G, Yaffe D (1971) Alterations of enzymatic activities during muscle differentiation in vitro. Dev Biol 25:1–29
29. Yablonka Z, Yaffe D (1977) Synthesis of myosin light chains and accumulation of translatable mRNA coding for light chain-like polypeptides in differentiating muscle cultures. Differentiation 8:133–143
30. Chargé SB, Rudnicki MA (2004) Cellular and molecular regulation of muscle regeneration. Physiol Rev 84:209–238
31. Gonzalez I, Tripathi G, Carter EJ, Cobb LJ, Salih DA, Lovett FA, Holding C, Pell JM (2004) Akt2, a novel functional link between p38 mitogen-activated protein kinase and phosphatidylinositol 3-kinase pathways in myogenesis. Mol Cell Biol 24:3607–3622
32. Manning BD, Cantley LC (2007) AKT/PKB signaling: navigating downstream. Cell 129:1261–1274
33. Chao DT, Korsmeyer SJ (1998) BCL-2 family: regulators of cell death. Annu Rev Immunol 16:395–419
34. Bornman L, Polla BS, Lotz BP, Gericke GS (1995) Expression of heat-shock/stress proteins in Duchenne muscular dystrophy. Muscle Nerve 18:23–31
35. Lanneau D, de Thonel A, Maurel S, Didelot C, Garrido C (2007) Apoptosis versus cell differentiation: role of heat shock proteins HSP90, HSP70 and HSP27. Prion 1:53–60
36. Schneider C, Sepp-Lorenzino L, Nimmesgern E, Ouerfelli O, Danishefsky S, Rosen N, Hartl FU (1996) Pharmacologic shifting of a balance between protein refolding and degradation mediated by Hsp90. Proc Natl Acad Sci 93:14536–14541
37. Shaknovich R, Shue G, Kohtz DS (1992) Conformational activation of a basic helix-loop-helix protein (MyoD1) by the C-terminal region of murine HSP90 (HSP84). Mol Cell Biol 12:5059–5068
38. Rotwein P, Wilson EM (2009) Distinct actions of Akt1 and Akt2 in skeletal muscle differentiation. J Cell Physiol 219:503–511
39. Wilson EM, Rotwein P (2007) Selective control of skeletal muscle differentiation by Akt1. J Biol Chem 282:5106–5110
40. Yun BG, Matts RL (2005) Hsp90 functions to balance the phosphorylation state of Akt during C2C12 myoblast differentiation. Cell Signal 17:1477–1485
41. Stephens L, Anderson K, Stokoe D, Erdjument-Bromage H, Painter GF, Holmes AB, Gaffney PR, Reese CB, McCormick F, Tempst P, Coadwell J, Hawkins PT (1998) Protein kinase B kinases that mediate phosphatidylinositol 3, 4, 5-trisphosphate-dependent activation of protein kinase B. Science 279:710–714
42. Sarbassov DD, Guertin DA, Ali SM, Sabatini DM (2005) Phosphorylation and regulation of Akt/PKB by the rictor-mTOR complex. Science 307:1098–1101
43. Testa JR, Bellacosa A (2001) AKT plays a central role in tumorigenesis. Proc Natl Acad Sci 98:10983–10985
44. Fujita N, Sato S, Ishida A, Tsuruo T (2002) Involvement of Hsp90 in signaling and stability of 3-phosphoinositide-dependent kinase-1. J Biol Chem 277:10346–10353
45. Sato S, Fujita N, Tsuruo T (2000) Modulation of Akt kinase activity by binding to Hsp90. Proc Natl Acad Sci 97:10832–10837
46. Shiota C, Woo JT, Lindner J, Shelton KD, Magnuson MA (2006) Multiallelic disruption of the rictor gene in mice reveals that mTOR complex 2 is essential for fetal growth and viability. Dev Cell 11:583–589
47. Weston CR, Davis RJ (2007) The JNK signal transduction pathway. Curr Opin Cell Biol 19:142–149
48. Gallo KA, Johnson GL (2002) Mixed-lineage kinase control of JNK and p38 MAPK pathways. Nat Rev Mol Cell Biol 3: 663–672
49. Rana A, Gallo K, Godowski P, Hirai S, Ohno S, Zon L, Kyriakis JM, Avruch J (1996) The mixed lineage kinase SPRK phosphorylates and activates the stress-activated protein kinase activator, SEK-1. J Biol Chem 271:19025–19028
50. Merritt SE, Mata M, Nihalani D, Zhu C, Hu X, Holzman LB (1999) The mixed lineage kinase DLK utilizes MKK7 and not MKK4 as substrate. J Biol Chem 274:10195–10202
51. Vasilevskaya IA, Rakitina TV, O'Dwyer PJ (2003) Geldanamycin and its 17-allylamino-17-demethoxy analogue antagonize the action of Cisplatin in human colon adenocarcinoma cells: differential caspase activation as a basis for interaction. Cancer Res 63:3241–3246
52. Kluck RM, Bossy-Wetzel E, Green DR, Newmeyer DD (1997) The release of cytochrome c from mitochondria: a primary site for Bcl-2 regulation of apoptosis. Science 275:1132–1136
53. Yang J, Liu X, Bhalla K, Kim CN, Ibrado AM, Cai J, Peng TI, Jones DP, Wang X (1997) Prevention of apoptosis by Bcl-2: Release of cytochrome c from mitochondria blocked. Science 275:1129–1132
54. Susin SA, Zamzami N, Castedo M, Hirsch T, Marchetti P, Macho A, Daugas E, Geuskens M, Kroemer G (1996) Bcl-2 inhibits the

mitochondrial release of an apoptogenic protease. J Exp Med 184:1331–1342
55. Yoshida N, Yoshida S, Koishi K, Masuda K, Nabeshima Y (1998) Cell heterogeneity upon myogenic differentiation: down-regulation of MyoD and Myf-5 generates 'reserve cells'. J Cell Sci 111:769–779
56. Nagata Y, Kobayashi H, Umeda M, Ohta N, Kawashima S, Zammit PS, Matsuda R (2006) Sphingomyelin levels in the plasma membrane correlate with the activation state of muscle satellite cells. J Histochem Cytochem 54:375–384
57. Dominov JA, Dunn JJ, Miller JB (1998) Bcl-2 expression identifies an early stage of myogenesis and promotes clonal expansion of muscle cells. J Cell Biol 142:537–544
58. Füchtbauer EM, Westphal H (1992) MyoD and myogenin are coexpressed in regenerating skeletal muscle of the mouse. Dev Dyn 193:34–39
59. Halevy O, Novitch BG, Spicer DB, Skapek SX, Rhee J, Hannon GJ, Beach D, Lassar AB (1995) Correlation of terminal cell cycle arrest of skeletal muscle with induction of p21 by MyoD. Science 267:1018–1021
60. Lassar AB, Davis RL, Wright WE, Kadesch T, Murre C, Voronova A, Baltimore D, Weintraub H (1991) Functional activity of myogenic HLH proteins requires hetero-oligomerization with E12/E47-like proteins in vivo. Cell 66:305–315
61. Davis RL, Cheng P, Lassar AB, Weintraub H (1990) The MyoD DNA binding domain contains a recognition code for muscle specific gene activation. Cell 60:733–746
62. Kayani AC, Close GL, Broome CS, Jackson MJ, McArdle A (2008) Enhanced recovery from contraction-induced damage in skeletal muscles of old mice following treatment with the heat shock protein inducer 17-(allylamino)-17-demethoxygeldanamycin. Rejuvenation Res 11:1021–1030
63. McArdle A, Dillmann WH, Mestril R, Faulkner JA, Jackson MJ (2004) Overexpression of HSP70 in mouse skeletal muscle protects against muscle damage and age-related muscle dysfunction. FASEB J 18:355–357
64. Senf SM, Dodd SL, McClung JM, Judge AR (2008) Hsp70 overexpression inhibits NF-kappaB and Foxo3a transcriptional activities and prevents skeletal muscle atrophy. FASEB J 22: 385–3836
65. Bakkar N, Wang J, Ladner KJ, Wang H, Dahlman JM, Carathers M, Acharyya S, Rudnicki MA, Hollenbach AD, Guttridge DC (2008) IKK/NF-kappaB regulates skeletal myogenesis via a signaling switch to inhibit differentiation and promote mitochondrial biogenesis. J Cell Biol 180:787–802
66. Luo S, Zhang B, Dong XP, Tao Y, Ting A, Zhou Z, Meixiong J, Luo J, Chiu FC, Xiong WC, Mei L (2008) HSP90 beta regulates rapsyn turnover and subsequent AChR cluster formation and maintenance. Neuron 60:97–110
67. Lin W, Burgess RW, Dominguez B, Pfaff SL, Sanes JR, Lee KF (2001) Distinct roles of nerve and muscle in postsynaptic differentiation of the neuromuscular synapse. Nature 410:1057–1064
68. Donnelly A, Blagg BSJ (2008) Novobiocin and additional inhibitors of the Hsp90 C-Terminal nucleotide-binding pocket. Curr Med Chem 15:2702–2717
69. Neckers L (2002) Hsp90 inhibitors as novel cancer chemotherapeutic agents. Trends Mol Med 8:S55–S61
70. Schulte TW, Neckers LM (1998) The benzoquinone ansamycin 17-allylamino-17-demethoxygeldanamycin binds to HSP90 and shares important biologic activities with geldanamycin. Cancer Chemother Pharmacol 42:273–279
71. Holzbeierlein JM, Windsperger A, Vielhauer G (2010) Hsp90: a drug target? Curr Oncol Rep 12:95–101

Neuroscience Research 70 (2011) 189–196

Contents lists available at ScienceDirect

Neuroscience Research

journal homepage: www.elsevier.com/locate/neures

Relationship of negative mood with prefrontal cortex activity during working memory tasks: An optical topography study

Ryuta Aoki[a,b,*], Hiroki Sato[c,**], Takusige Katura[c], Kei Utsugi[d], Hideaki Koizumi[c], Ryoichi Matsuda[a], Atsushi Maki[c]

[a] Department of Life Sciences, Graduate School of Arts and Sciences, The University of Tokyo, 3-8-1 Komaba, Meguro-ku, Tokyo 153-8902, Japan
[b] Japan Society for the Promotion of Science, 8 Ichibancho, Chiyoda-ku, Tokyo 102-8472, Japan
[c] Advanced Research Laboratory, Hitachi, Ltd., 2520 Akanuma, Hatoyama, Saitama, 350-0395, Japan
[d] Systems Development Laboratory, Hitachi, Ltd., 292 Yoshida-cho, Totsuka-ku, Yokohama, Kanagawa 244-0817, Japan

ARTICLE INFO

Article history:
Received 15 December 2010
Received in revised form 24 February 2011
Accepted 25 February 2011
Available online 5 March 2011

Keywords:
Emotion–cognition interaction
Prefrontal cortex
Near-infrared spectroscopy (NIRS)
Optical topography
Profile of Mood States (POMS)

ABSTRACT

Mood has a substantial impact on cognitive functions. Although studies have shown that the interaction between mood and cognition is mediated by the prefrontal cortex (PFC), little is known about how naturalistic mood in everyday life is associated with PFC activity during cognitive tasks. We investigated whether inter-individual variation in perceived mood under current life situations (recent week) is related to PFC activity during working memory (WM) tasks in healthy adults. Levels of positive and negative moods were quantified with the Profile of Mood States (POMS) questionnaire. PFC activities during verbal and spatial WM tasks were measured by optical topography (OT), a non-invasive low-constraint neuroimaging tool, to minimize experimental intervention in participants' moods. Group-average analysis showed significant activations in the bilateral dorsolateral PFC in both WM tasks. Correlation analysis revealed that the participants reporting higher levels of negative moods showed lower levels of PFC activity during the verbal WM task but not during the spatial WM task. This relationship was significant even after controlling for possible confounding factors such as age, gender, and task performance. Our results suggest that verbal WM is linked with naturalistic negative mood and that the PFC is involved in the mood–cognition interaction in daily circumstances.

1. Introduction

In everyday life, the way we think and act is substantially affected by our mood, regardless of whether we recognize it or not. Psychologists have long investigated the relationship between mood and cognition, revealing that many cognitive functions are actually modulated by mood (Mitchell and Phillips, 2007; Robinson and Sahakian, 2009). An important cognitive function in the mood-cognition interaction is working memory (WM), a mental process well documented in both psychology and neuroscience (Baddeley, 2003). Behavioral studies have shown that performance on various cognitive tasks requiring WM (e.g., word span task, Tower of London planning task) is affected by the participant's mood Mitchell and Phillips (2007). Psychopharmacological studies and theoretical models have also suggested that mood and relevant neurotransmitters (e.g., dopamine and serotonin) are linked with WM performance (Ashby et al., 1999; Luciana et al., 1998).

Neuroimaging research has begun to elucidate the underlying neural mechanisms of the mood-cognition interaction in WM. As the prefrontal cortex (PFC) has been demonstrated to play a crucial role in WM (Smith and Jonides, 1999; Smith et al., 1996), the effect of mood on WM is likely mediated by the PFC function. Indeed, a functional magnetic resonance imaging (fMRI) study showed that activity in the dorsolateral PFC (DLPFC) during a WM task (numerical N-back task) was reduced when the participants were exposed to acute psychological stress (induced by viewing aversive movie clips), which led to increased negative mood (Qin et al., 2009). This finding is consistent with the results of other fMRI studies showing that WM-related activity in the DLPFC is attenuated by affective modulation using negative emotional stimuli (Anticevic et al., 2010; Perlstein et al., 2002). These results provide valuable insight into the role of the PFC in the interaction between mood and WM.

However, experimentally induced mood may be different from naturalistic mood in its relationship with cognition. Characteristics of induced moods (e.g., intensity, duration, and whether

* Corresponding author. Tel.: +81 3 5454 6637; fax: +81 3 5454 4306.
** Co-corresponding author. Tel.: +81 49 296 6111; fax: +81 49 296 5999.
E-mail addresses: cc097702@mail.ecc.u-tokyo.ac.jp, ryuta.aoki.mu@hitachi.com (R. Aoki), hiroki.sato.ry@hitachi.com (H. Sato).

0168-0102/$ – see front matter © 2011 Elsevier Ireland Ltd and the Japan Neuroscience Society. All rights reserved.
doi:10.1016/j.neures.2011.02.011

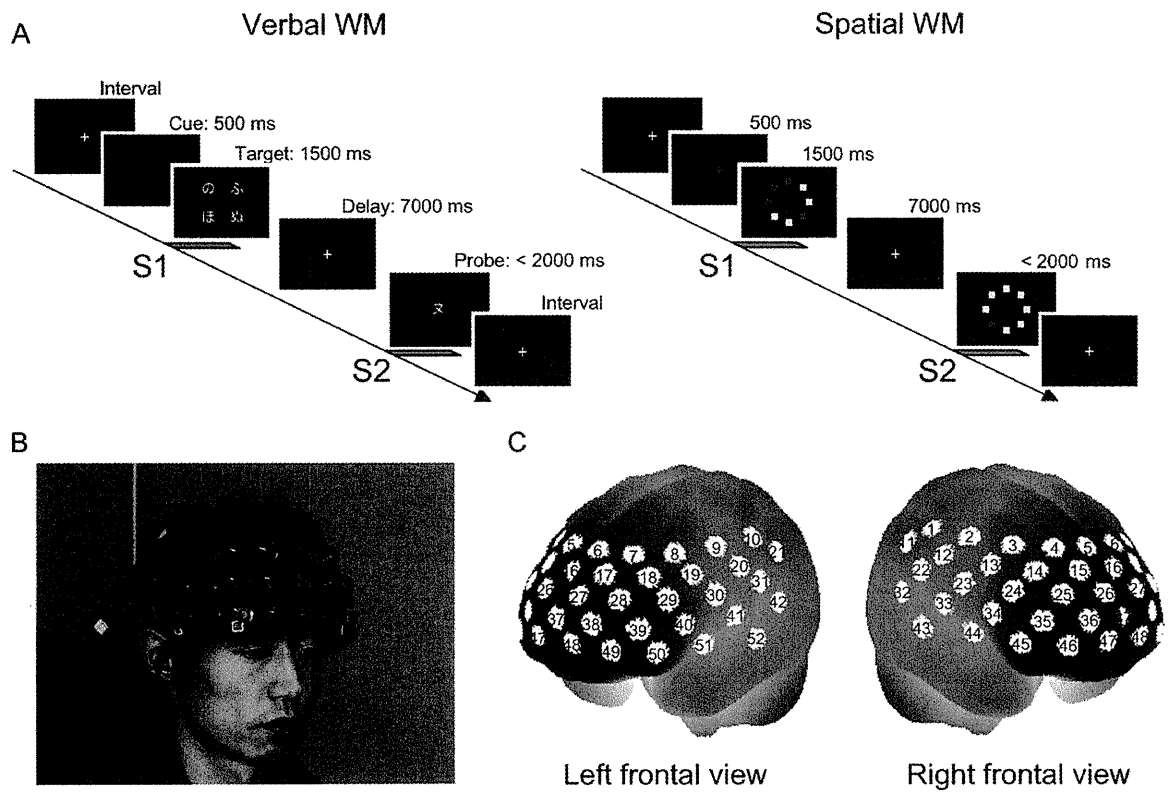

Fig. 1. Task paradigm and experimental setting. (A) Schematic diagrams of verbal and spatial WM tasks. Participants were instructed to remember the target stimuli (S1) and to report whether the character (verbal WM task) or location of a red square (spatial WM task) presented in the probe stimuli (S2) was identical to one of the items in S1. (B) OT probe-holder worn by participant. A 3 × 11 probe array (17 light sources and 16 detectors) was positioned on the forehead. (C) Arrangement of measurement positions (52 channels) in MNI space, which was estimated by means of probabilistic registration method (Singh et al., 2005).

the demand effect exists) depend on various methods of mood induction procedures (Martin, 1990) and may differ qualitatively from those of naturalistic moods. Indeed, a previous study demonstrated that induced moods and naturalistic moods can occasionally exert different, or even opposite, effects on certain aspects of cognitive functions (Parrot and Sabini, 1990). To understand the mood-cognition interaction more thoroughly, evidence from both induced and naturalistic moods should be converged (Mayer et al., 1995). Thus, the relationship between naturalistic mood and WM is worth investigating in neuroimaging studies, in addition to previous research using affective modulation paradigms.

In this study, we investigated whether and how naturalistic moods in healthy adults are associated with PFC activity during WM tasks. We used individual differences (Kosslyn et al., 2002), which enable exploring the relationship between mood and brain activity without any explicit mood induction. Specifically, we tested whether inter-individual variations in the levels of positive or negative moods are correlated with PFC activity in response to the WM tasks. Participants' naturalistic moods in their current life (the last week) were assessed with the Profile of Mood States (McNair et al., 1971; Yokoyama et al., 1990), a self-report questionnaire used in previous studies that examined the PFC role in the mood-cognition interaction (Canli et al., 2004; Harrison et al., 2009). PFC activity during WM tasks was measured with optical topography (OT), a non-invasive, low-constraint neuroimaging technique, to minimize the mood modulation due to the experiment. OT enables measuring hemodynamic responses in the cerebral cortex under near-natural situations (e.g., sitting position) (Maki et al., 1995; Tsujimoto et al., 2004) and can tap into relationships between naturalistic mood and PFC activity (Suda et al., 2009; Suda et al., 2008). We used two types of WM tasks (verbal and spatial) that had an identical delayed-response paradigm, a standard cognitive activation paradigm often used in the human neuroimaging studies of WM (Smith and Jonides, 1999; Smith et al., 1996).

2. Materials and methods

2.1. Participants

Thirty-two healthy adults participated in the experiment after they provided written informed consent. Their handedness was assessed with the Edinburgh Handedness Inventory (Oldfield, 1971), and data from a female who demonstrated left-handedness were excluded from the analysis. Data from two other females were also excluded from the analysis because of their poor behavioral performance (<50% correct responses for the spatial WM tasks). The remaining 29 participants (12 females, 17 males, mean age = 35.9 years, SD = 7.7, and range = 25–58, all right handed) were included in the final analysis. The study was approved by the Ethics Committee of Hitachi, Ltd.

2.2. Mood assessment

The participants' naturalistic moods were assessed by means of a short form of the Profile of Mood States (McNair et al., 1971), which has been translated and validated for the Japanese general population (Yokoyama et al., 1990). McNair et al. (1971) defined moods as mild, pervasive, and generalized affective states that are perceived subjectively by individuals. The participants rated 30 mood-related adjectives on a 5-point scale ranging from 0 ("not at all") to 4 ("extremely") on the basis of how they had been feeling during the past week. While the POMS consists of six identifiable mood factors (tension, depression, anger, vigor, fatigue, and confusion), our study focused on the POMS positive mood score (the score of vigor subscale) and the POMS negative mood score (the sum of the score for the other five subscales), following a previous study (Canli et al., 2004).

2.3. WM tasks

The tasks were presented through software, the Platform of Stimuli and Tasks (developed by Hitachi, ARL). Each participant performed two types of WM tasks (verbal and spatial), which had an identical delayed-response paradigm (Fig. 1A). In both tasks, each trial started with a 1500-ms presentation of the target stimuli (S1), which was followed by a delay of 7000 ms. A probe stimulus (S2) was then presented for 2000 ms or until the participant responded. The intervals between S2 onset and the following S1 onset in the next trial were randomized from 16 to 24 s. Only a

fixation cross was presented during the interval and the delay period. In addition, a visual cue (changing the color of the fixation cross) was presented for 500 ms prior to trial onset. Auditory cues (1000 and 800 Hz pure tones of 100-ms duration) were presented at the onsets of the visual cue and S2, respectively.

In the verbal WM task, four Japanese characters in *Hiragana* were presented as S1, and a Japanese character in *Katakana* was presented as S2. The participants were instructed to judge whether the character presented as S2 corresponded to any of the characters in S1 and then to press the appropriate button. Because the characters in S1 and S2 were presented in different Japanese morphograms (i.e., *Hiragana*/*Katakana*), participants were prompted to make their judgments based on the phonetic information of the characters, not by their form. In the spatial WM task, S1 was the location of four red squares out of eight locations, and S2 was the location of a red square. The participants' task was to assess if the location of the red square presented as S2 was identical to any of the locations of the four red squares presented in S1.

Each WM task had two additional conditions: Eriksen flanker tasks (Eriksen and Eriksen, 1974) were embedded in the delay period as distracter stimuli. These conditions were irrelevant to the purpose of the present study, so they were not included in the analysis.

2.4. Procedure

Participants were seated in a comfortable chair in a dim, quiet room. Their moods were assessed with a short form of the POMS questionnaire (Japanese version) (Yokoyama et al., 1990) at the beginning of the experiment. Next, they received computer-automated instructions that were followed by a brief practice session to familiarize them with the tasks. Thereafter, OT measurements were conducted while the participants performed the WM tasks. The tasks were organized into two sessions, one for the verbal WM task and the other for the spatial WM task, with a counterbalanced order across participants. Each session included five trials of either one of the tasks, and the sessions were separated by a short break (approximately 1 min). After the measurements, the participants completed a brief questionnaire that assessed their feelings about the experiments, which included subjective ratings of task difficulty on a 5-point scale, ranging from 1 ("not at all") to 5 ("extremely"). The duration of the OT measurements was approximately 15 min, and the whole experiment took about 45 min.

2.5. OT measurement

We used an OT system (ETG-4000, Hitachi Medical Corporation, Japan) equipped with 17 near-infrared light sources and 16 detectors. The light sources consisted of near-infrared continuous laser diodes with two wavelengths of 695 and 830 nm. The transmitted light was detected every 100 ms with avalanche photodiodes located 30 mm from the sources. These optodes (i.e., sources and detectors) were arrayed in a 3×11 lattice pattern and embedded in a soft silicon holder that was placed on the participant's forehead (Fig. 1B). This configuration formed 52 measurement points (defined as channels (Chs)), corresponding to each source-detector pair (Fig. 1C). The average power of each light source was 2 mW (for both wavelengths), and the sources were modulated at different frequencies (1–10 kHz) for wavelengths and sources so that signals from different measurement points could be discriminated.

To estimate the locations of the OT channels in the Montreal Neurological Institute (MNI) space and to generate 3-D topographical maps (Figs. 2 and 3), we used the probabilistic registration method (Okamoto and Dan, 2005; Singh et al., 2005). Prior to the experiment, we corrected the sample data for the three-dimensional coordinates of the 33 optode locations and scalp landmarks (in accordance with the international 10–20 system: Fp1, Fp2, Fz, T3, T4, C3, C4) for eight volunteers. The data were recorded with a 3D-magnetic space digitizer (3D probe positioning unit for OT system, EZT-DM101, Hitachi Medical Corporation, Japan).

2.6. Data analysis

Analyses were performed by means of plug-in-based analysis software, Platform for Optical Topography Analysis Tools (developed by Hitachi, ARL; run on MATLAB, The MathWorks, Inc., U.S.A.). First, we calculated the relative values of hemoglobin concentration changes (Hb-signals for oxy-Hb and deoxy-Hb) for each channel on the basis of the modified Beer-Lambert law, using light signals transmitted at the two wavelengths. The time-continuous data of Hb-signals for each channel were separated into task blocks, which were defined as a 25.5-s period starting from 1.0 s before S1 onset and ending 16.0 s after S2 onset, each containing a WM task trial. Next, blocks contaminated by motion artifacts were discarded. Although previous OT studies have used various methods to detect motion artifacts, no established method has been developed. Some studies used subjective methods based on visual inspection (Minagawa-Kawai et al., 2011), whereas others used objective methods (Orihuela-Espina et al., 2010; Takizawa et al., 2008). In this study, we used a criterion similar to (Pena et al., 2003): an oxy-Hb signal change larger than 0.4 mM mm over two successive samples (during 200 ms) was defined as a motion artifact. We found that this criterion effectively detected sharp noises (putatively unphysiological signal changes) identified by a visual inspection in our data, while maintaining the rejection rate at a low level (4.9%). The remaining data were baseline-corrected by linear regression based on the least squares method by using the data for the first 1.0 s the last 4.0 s of each block.

To evaluate the PFC activity during the tasks, we determined the '*activation period*' as being 3.5 s starting 5.0 s after S1 onset and ending on S2 onset (Fig. 2C). The onset of the activation period (5.0 s after S1 onset) was determined by taking into consideration the delay in hemodynamic changes from the neuronal activity. The offset of the activation period (immediately before S1 onset) was selected to avoid any confounding effects related to S2 presentation and the participant's response to the task. Because the activation period was entirely included in the 7.0-s WM-delay period, we expected that Hb-signals during this period would reflect cortical activity related to WM functions (i.e., encoding and maintenance) without it being affected by activity related to visual stimulation due to S2 or by body movement due to pressing buttons. Note that this time window was determined *a priori* and that the results reported here were not changed when we selected a longer time period (e.g., 5.0-s period starting 5.0 s after S1 onset; See Supplementary Fig. S1). The mean signal changes during the activation period, termed '*activation values*,' were calculated for both oxy-Hb and deoxy-Hb signals for each block. To assess the statistical significance of Hb-signal changes for the tasks, we first averaged the activation values within participants then performed a *t*-test (one sample, one-tailed) of the individual activation values against 0 across participants. For the between-task comparison of the activation values, we used a paired *t*-test (two-tailed) across participants.

To analyze the relationships of mood with task performance and PFC activity, we calculated the correlations between the POMS scores and behavioral measures or oxy-Hb signal changes for both WM tasks. We used Spearman's rank correlation because the relationships of subjective ratings with behavioral and neural measures are not necessarily regarded as linear (Schroeter et al., 2004).

All of these statistical analyses were performed for each channel. Therefore, when creating the statistical parametric map consisting of 52 channels, we used the false discovery rate (FDR) method to correct for multiple comparisons (Singh and Dan, 2006) with a threshold of FDR (q) < 0.05. Because FDR correction set a statistical threshold for each analysis, uncorrected *P*-values at thresholds were different across maps. Thus, the ranges of the statistical values (Student's *t* and Spearman's *r*, together with the thresholds of the uncorrected *P*-values) for the significant channels are presented for each statistical parametric map. Note that *P* denotes the uncorrected *P*-values for each channel and that *q* denotes the FDR for each map throughout this paper.

3. Results

3.1. POMS scores and subjective ratings

The mean and standard deviation (SD) of the POMS positive mood scores and negative mood scores were 8.76 ± 2.89 (ranging from 5 to 16) and 24.8 ± 14.5 (ranging from 3 to 56), respectively. These results are comparable to those obtained for a large sample of healthy Japanese adults (Yokoyama et al., 1990). The scores for male (9.18 ± 3.38 for positive mood scores, 22.8 ± 15.2 for negative mood scores) and female (8.17 ± 2.00 for positive mood scores, 27.6 ± 13.5 for negative mood scores) participants were not significantly different ($P = 0.556$ for positive mood scores, $P = 0.370$ for negative mood scores; Mann–Whitney *U*-test). The POMS positive mood scores and negative mood scores were not significantly correlated ($r = -0.28$, $P = 0.136$; Spearman's rank correlation).

The subjective ratings of task difficulty were 2.62 ± 0.90 for the verbal WM task and 2.93 ± 1.13 for the spatial WM task. The between-task difference was not significant ($P = 0.079$, Wilcoxon signed-rank test).

3.2. Behavioral performances

The mean reaction time (RT) for correct responses within individual participants was calculated for each WM task. The across-participants' mean and SD for RT were 1380 ± 239 ms for the verbal WM task and 1475 ± 270 ms for the spatial WM task. There were no significant differences between tasks ($t = -1.66$, $P = 0.108$, two-tailed paired *t*-test).

The number of correct responses ranged from three to five for both tasks, and the across-participants' mean and SD were 4.72 ± 0.59 for the verbal WM task and 4.31 ± 0.66 for the spatial WM task. Although this difference was relatively small (0.41), it was statistically significant ($P = 0.018$, Wilcoxon signed-rank test).

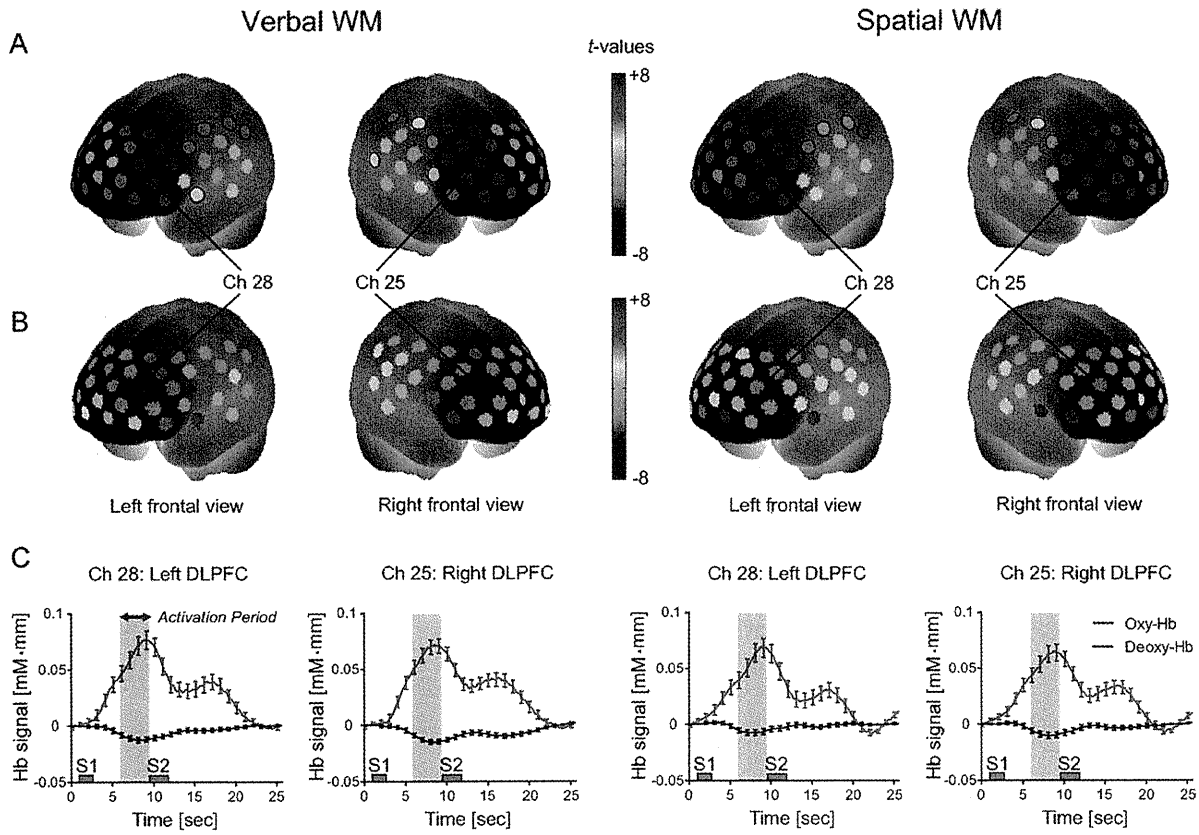

Fig. 2. Hemodynamic changes during verbal and spatial WM tasks. (A) Activation *t*-maps of oxy-Hb signal increase. (B) Activation *t*-maps of deoxy-Hb signal decrease. The Student's *t*-value is indicated by a color scale for each channel. Channels with significant *t*-values are marked with circles (FDR $q < 0.05$). (C) Time courses for Hb-signal changes for representative channels (Chs 25 and 28 for right and left hemispheres, respectively). These time courses represent the grand average (with standard error bars) across all participants. The time spans (green bars perpendicular to *x*-axis) indicate activation period (3.5-s duration). Small rectangles (gray) indicate stimuli presentation time (S1, S2).

To determine whether participants' moods were associated with task performance, we calculated the correlation coefficients (Spearman's *r*) between the POMS scores and behavioral measures (accuracy and RT). A significant correlation was found only in the relationship between the POMS negative mood scores and RT for the verbal WM ($r = -0.37$, $P = 0.046$), although this relationship was no longer significant after controlling for participants' age and gender ($r = -0.29$, $P = 0.141$). No other significant correlation was evident between the POMS scores and behavioral measures ($r = -0.26$ to 0.20, $P > 0.174$; see Supplementary Table).

3.3. PFC activity during WM tasks

First, we examined the across-participants' mean of the activation values for each WM task, without considering individual differences in the mood scores.

For both tasks, significant increases in the oxy-Hb signals (FDR $q < 0.05$) were observed in a broad region of the PFC (Fig. 2A). For the verbal WM task, the oxy-Hb signals increased for 39 channels ($t = 1.97$ to 6.55, $P < 0.030$, $q < 0.05$). Similarly, for the spatial WM task, the oxy-Hb signals increased for 36 channels ($t = 2.10$ to 6.52, $P < 0.024$, $q < 0.05$).

Decreases in the deoxy-Hb signals were observed in a more localized region (Fig. 2B). For the verbal WM task, significant deoxy-Hb signal decreases were observed for five channels (Chs 25, 28, 18, 4, and 7; $t = -5.17$ to -3.03, $P < 0.003$, $q < 0.05$), two for the right hemisphere (Chs 4 and 25), and three for the left hemisphere (Chs 7, 18, and 28). The deoxy-Hb signal decreases for the spatial WM task were not significant at the FDR-corrected threshold. However, for reference, we found considerable decreases in the deoxy-Hb signals for the five channels (Chs 25, 18, 4, 8, and 28; $t = -2.82$ to -1.71, $P < 0.05$ but $q > 0.05$), two for the right hemisphere (Chs 4 and 25), and three for the left hemisphere (Chs 8, 18, and 28).

A comparison of the activation values between the verbal and spatial WM tasks revealed no significant differences in either the oxy-Hb signal increases or the deoxy-Hb signal decreases ($q > 0.05$).

3.4. Temporal characteristics of oxy-Hb signal change

We analyzed the temporal characteristics of the oxy-Hb signal change based on the grand-averaged time course (Fig. 2C). For the channels where the oxy-Hb signal increases were significant during the activation period, the time courses for the oxy-Hb signal change had two peaks. The first (and the maximum) peak was observed during the delay period, and the second, more modest peak was observed after S2 was presented. We calculated the peak latency for the first peak, which was defined as the duration from S1 onset to the time the oxy-Hb signal reached a maximal value, and averaged this across channels with a significant oxy-Hb signal increase for both WM tasks. The mean of the peak latency was 7.81 ± 0.90 s for the verbal WM task and 7.61 ± 1.08 s for the spatial WM task. The difference between tasks was not significant ($t = 1.82$, $df = 35$, $P = 0.077$, two-tailed paired *t*-test).

3.5. Correlation of POMS score with PFC activity

Next, to examine how the participants' moods were associated with the PFC activity during each WM task, we analyzed the correlation (Spearman's rank correlation) between the POMS scores

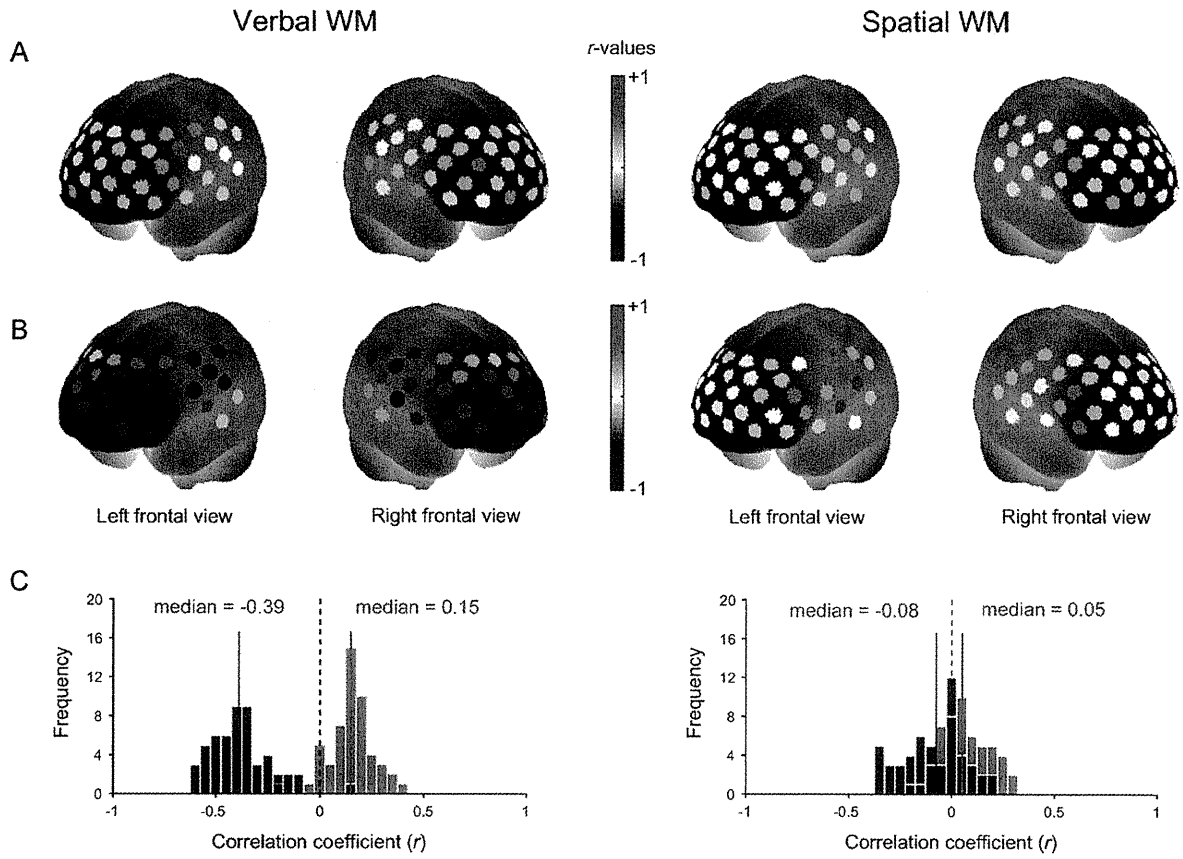

Fig. 3. Correlation between POMS scores and oxy-Hb signals. (A) Correlation *r*-maps showing relationship between POMS positive mood scores and oxy-Hb signal increase. (B) Correlation *r*-maps showing relationship between POMS negative mood scores and oxy-Hb signal increase. Left pairs: verbal WM task, right pairs: spatial WM task. The correlation coefficient (Spearman's *r*) is indicated by a color scale for each channel. Channels with statistical significance are marked with circles (FDR $q < 0.05$). (C) Histograms illustrate distributions of *r*-values for each *r*-map (Left: verbal WM, right: spatial WM). The vertical line indicates the median *r*-value among 52 channels consisting of a map. Red: correlation with POMS positive mood score, blue: correlation with POMS negative mood score.

and the activation values. We used only the oxy-Hb signal change because the deoxy-Hb signals did not show clear changes compared to the oxy-Hb signals (as described before).

For the verbal WM task, the oxy-Hb signal changes during the task tended to be positively correlated with the POMS positive mood scores (median *r*-value = 0.15, ranging from −0.21 to 0.40), whereas negatively correlated with the POMS negative mood scores (median *r*-value = −0.39, ranging from −0.62 to 0.16) (Fig. 3). We found statistically significant negative correlations between the POMS negative mood scores and the oxy-Hb signal changes for 19 channels ($r = -0.62$ to -0.44, $P = 0.0006$ to 0.017, $q < 0.05$) (Fig. 3B). Notably, the partial correlation analysis showed that a significant correlation remained in a specific channel (Ch 28; $r = -0.62$, $P = 0.0009$, $q < 0.05$) even when the participants' age, gender, and task performance (accuracy and RT) were controlled for. In addition, the correlation coefficients for the male ($n = 17$) and female ($n = 12$) participants were not significantly different in this channel ($r = -0.49$ for males, $r = -0.53$ for females; $P = 0.913$, Fisher's *Z*-test). The correlation plot for Ch 28 is shown in Fig. 4.

For the spatial WM task, the oxy-Hb signal changes during the task did not significantly correlate with either the POMS positive mood scores ($r = -0.20$ to 0.30, $P > 0.116$, $q > 0.05$) or negative mood scores ($r = -0.37$ to 0.21, $P > 0.056$, $q > 0.05$).

We also examined the correlations between task performance (accuracy and RT) and the oxy-Hb signal changes. Although there was a weak trend that higher accuracy was associated with a larger oxy-Hb increase in the frontopolar region for both verbal and spatial WM tasks ($r < 0.35$), no significant relationship was found (Supplementary Fig. S2).

4. Discussion

We measured the PFC activity during verbal and spatial WM tasks under low-constraint, near-natural conditions by using OT,

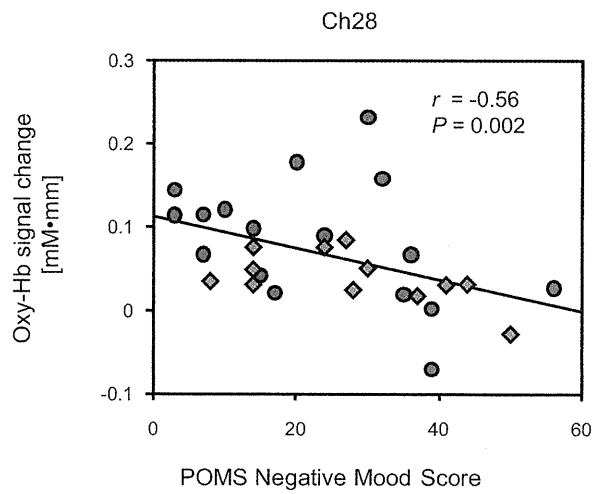

Fig. 4. Scatter plot showing relationship between POMS negative mood scores and PFC activity during verbal WM task in Ch 28. The negative correlation between the POMS scores and PFC activity was significant (FDR $q < 0.05$) in this channel, even after controlling for age, gender, and task performance. The blue circles indicate male participants, and the red diamonds indicate female participants. *r*: Spearman's rank correlation coefficient, *P*: uncorrected value. (For interpretation of the color information in this figure legend, the reader is referred to the web version of the article.)

to investigate the relationships between naturalistic mood and PFC activity. The results revealed statistically significant negative correlations between the POMS negative mood scores and PFC activity during the verbal WM task, whereas the opposite tendency was found for the POMS positive mood scores. However, the PFC activity during the task was not significantly correlated with either the POMS positive or negative mood scores for the spatial WM task. Our results indicate that even a normal range of mood variation in healthy individuals is associated with PFC activity during a WM task, suggesting a mood-cognition interaction under everyday circumstances manifested in PFC activity.

4.1. PFC activity induced by WM tasks

We observed a significant oxy-Hb signal increase in the PFC region in response to both verbal and spatial WM tasks. We did not observe a clear deoxy-Hb signal decrease comparable to the oxy-Hb signal increase, probably due to the lower signal to noise ratio. The decrease in the deoxy-Hb signal was significant only for the verbal WM task, but a similar spatial pattern was observed for the spatial WM task (Fig. 2B). An oxy-Hb signal increase accompanied by a deoxy-Hb signal decrease is considered to be a typical pattern of a hemodynamic response elicited by neuronal activity often observed in OT measurements (Herrmann et al., 2007; Sato et al., 2005, 1999). This pattern was found in the bilateral dorsolateral PFC, as identified by the probabilistic registration method (Okamoto and Dan, 2005; Singh et al., 2005). Therefore, we regarded these areas as activation foci responsible for WM functions. These results are consistent with those from previous research with other modalities (such as fMRI and PET), which have demonstrated DLPFC activation in response to performance of WM tasks (Gray et al., 2002; Smith and Jonides, 1999). Previous OT studies have also reported DLPFC activation during WM tasks (Hoshi et al., 2003; Tsujimoto et al., 2004). In particular, Tsujimoto et al. (2004), using the same delayed-response paradigm for the spatial WM task in our study, found that the oxy-Hb signal increase during the delay period was indeed WM-load dependent (two items vs. four items). This finding also supports that the PFC activity observed in our study can be regarded as WM related.

The PFC activity in response to the WM tasks was similar across the tasks not only in the spatial activation pattern (Fig. 2A and B) but also in the temporal characteristics (Fig. 2C), as shown by the analysis on peak latency. Although some previous studies found laterality in the PFC activity between verbal and spatial WM (Smith and Jonides, 1999; Smith et al., 1996) (i.e., relatively right dominant activation in spatial WM and left dominant activation in verbal WM), we did not observe significant differences in PFC activity between the tasks. One reason for this might be that we used a small number of trials for each condition, resulting in less sensitivity to differences in cortical responses between tasks. Whether OT can detect the lateralized PFC activity related to WM functions is a future issue to be investigated.

4.2. Relationship between negative mood and PFC activity associated with WM

We found a significant negative correlation between the POMS negative mood scores and the oxy-Hb signal increases—participants with higher levels of negative moods showed lower levels of PFC activity specifically during the verbal WM task. Of importance, this relationship was not explained by potential confounding factors such as age, gender, or task performance (i.e., accuracy and RT), as determined by partial correlation analysis. Particularly, the significant result in the partial correlation analysis was obtained in a channel located in the left DLPFC (Ch 28), where the WM-related activity (characterized by both the significant increase in the oxy-Hb signal and the significant decrease in the deoxy-Hb signal) was observed in the group-average analysis. Our results are consistent with the previous fMRI study by Qin et al. (2009), who reported that an induced negative mood attenuated DLPFC activity during a verbal WM task (numerical N-back task). The present study suggests that not only an induced negative mood but also a naturalistic negative mood is associated with PFC activity related to verbal WM function. Our results extend previous neuroimaging findings regarding the mood-cognition interaction to broader context under everyday circumstances: subjective moods during recent life situations are reflected in PFC activity responsive to cognitive tasks. The use of a low-constraint, less-stressful neuroimaging tool as well as a relatively short measurement time might have enabled us to probe the relationship between naturalistic mood and PFC activity sensitively.

We did not observe a significant association between performance (accuracy or RT) and mood scores or OT signals. Thus, it is unclear whether lower levels of PFC activity in participants reporting higher levels of negative moods indicate impoverished PFC reactivity to verbal WM or greater processing efficiency for verbal WM. However, we emphasize that our results are in line with previous OT studies showing that PFC activity during verbal fluency tasks is decreased in people who have higher levels of fatigue and sleepiness, apart from task performance (i.e., the effect of task performance on PFC activity was adjusted by multiple regression) (Suda et al., 2009, 2008). Collectively, these results including ours suggest that decreased PFC activity is a neural marker of higher negative mood (or lower motivation to engage in cognitive tasks), which could be more sensitive than behavioral measures. A more reliable relationship between behavioral measures and mood scores or PFC activity might be obtained if we increase the number of trials or use more difficult cognitive tasks.

One of the advantages of our study compared to the previous OT studies showing negative associations between PFC activity and levels of fatigue and sleepiness (Suda et al., 2009; Suda et al., 2008) is the use of a simple cognitive task, well described in the previous neuroimaging studies and requiring minimum motor responses. While verbal fluency tasks are useful tools for clinical research (Kameyama et al., 2006; Suto et al., 2004; Takizawa et al., 2008), these tasks involve many cognitive processes (e.g., word generation, verbal WM, and cognitive flexibility), making it difficult to characterize what aspects of cognitive processes are indeed relevant to decreased PFC activity associated with negative moods. Our study provides clearer evidence that the PFC is involved in the interaction between naturalistic mood and verbal WM.

We found a significant correlation between mood and PFC activity only for the verbal WM task but not for the spatial WM task. This result could imply that the relationship between mood and PFC activity differs across cognitive functions. Interestingly, some studies have reported that positive and negative moods are differently linked with verbal and spatial cognitive functions (Bartolic et al., 1999; Papousek et al., 2009). In these studies, performances on verbal fluency tasks were relatively worse than those on non-verbal (figural) fluency tasks in negative (dysphoric or withdrawal-related) moods, but opposite in positive (euphoric or approach-related) moods. These results are consistent with our results that showed the negative correlation between negative mood and PFC activity (as well as the trend of positive correlation between positive mood and PFC activity) if we interpret that higher PFC activity corresponds to better cognitive function (see Supplementary Fig. S2). Other studies using WM tasks also showed that verbal and spatial WM functions are selectively associated with experimentally induced positive or negative moods (Gray, 2001; Gray et al., 2002; Shackman et al., 2006). Considering these studies, our results suggest a specific interaction between negative mood and verbal WM under everyday circumstances.